THREE DIMENSIONAL EVALUATION OF THE TMJ CONDYLE POSITION IN DIFFERENT TYPES OF SKELETAL PATTERNS

By

Inês H. Guedes, DDS, MSc

A thesis submitted to the Faculty of Graduate Studies of

The University of Manitoba

In partial fulfillment of the requirements for the degree of

MASTER OF SCIENCE

Department of Preventive Dental Science

(Orthodontics)

University of Manitoba

Winnipeg

University of Manitoba

Faculty of Graduate Studies

The following certify that they have read the Master's thesis entitled:

"Three-dimensional evaluation of the TMJ condyle position in different types of skeletal patterns"

Submitted by

Dr. Inês H. Guedes

In partial fulfillment of the requirements for the degree of

Master of Science

Department of Preventive Dental Science

(Orthodontics)

Dr. Manuel Lagravere Vich (Supervisor), DDS, MSc, PhD, FRCD(C)

Department of Orthodontics, University of Alberta

Dr. Frank J. Hechter (Internal Examiner), DMD, MSc, PhD

Department of Preventive Dental Sciences, University of Manitoba

Dr. Mark G. Torchia (External Examiner), MS, PhD

Department of Surgery, University of Manitoba

Abstract

Objective: To evaluate three-dimensional position of the TMJ condyle within the glenoid fossa in different types of skeletal patterns.

Materials and methods: Ninety CBCT images were consecutively selected and divided into 3 groups (class I, class II and class III). The images were analyzed locating landmarks in the different areas of the condyle and glenoid fossa. All landmarks presented acceptable intra- (ICC and Cronbach's alpha = 0.99 to 1.00) and inter-rater reliability (ICC = 0.55 to 1.00; and Cronbach's alpha = 0.78 to 1.00). The mean values for anterior, superior and posterior joint space, condyle angle, fossa angle, and fossa depth were compared using ANOVA and Bonferroni post-hoc test ($p < 0.05$).

Results: There was a tendency for the anterior joint space (AJS) to be smaller than the posterior joint space (PJS) when the measurement means were evaluated. The mean absolute differences between AJS and PJS are as follows: class I left (0.97mm), class I right (1.25mm); class II left (0.5mm), class II right (1.27mm); class III left (0.87mm), class III right (0.7mm). Statistical analysis, however, evidenced no significant differences between the anterior, superior and posterior joint spaces between the different skeletal patterns or between sides.

Conclusion: There was no statistically significant difference in the three-dimensional position of the mandibular condyle in relation to the glenoid fossa in the different types of skeletal patterns studied. This shows that there was non-concentricity of the condyle for all the groups studied, and no particular direction was statistically significantly favored. It is unclear whether the differences found would be clinically significant, considering anatomical individual variations.

Keywords: temporomandibular joint, cone-beam computed tomography, three-dimensional analysis

Dedicatory

I would like to dedicate this work to my mom, my biggest supporter during the past 12 years of postsecondary education. Thanks for being my best friend every step of the way, without your unconditional love, encouragement and support I most definitely would not be here. *Obrigada por tudo mãezinha!*

Acknowledgments

I would like to sincerely thank the following individuals who have helped me throughout my graduate studies at the University of Manitoba:

- My supervisor, Dr. Manuel Lagravere, for his invaluable mentorship, patience, and incredible talent as a professor. I feel extremely blessed for having had the opportunity to working closely with such a skilled researcher in this project;
- My committee members, Dr. Frank Hechter and Dr. Mark Torchia for their revisions;
- The University of Alberta Orthodontic Graduate Program for kindly allowing me to use their patient and cone-beam CT database;
- All the University of Manitoba Graduate Orthodontic Clinic's full-time and part-time instructors for their mentorship, as well as the clinical and administrative support staff for their assistance during the past 36 months;
- My co-residents during the past three years, for all the good times we shared;
- Dr. Bruce McFarlane, Dr. Fred Murrell and the lovely Village Ortho staff for their kind encouragement;
- My Canadian family, Lisa and Delaney Lamont, for always being there for me;
- My dearest girlfriends, Maira, Rita, Sabrina, Roberta, Ligia, Liz and Marcella, for saying the right things, at the right times and always renewing my faith in myself;
- And lastly I want to thank my forever-safe harbor, my beautiful family - Ailson, Neide, Juliana, Binho, and little Lucas - for providing me with such a strong foundation of love, faith and encouragement during my orthodontic residency. I feel the luckiest girl for having you in my life.

Table of Contents

List of Tables

List of Figures

List of Abbreviations

2D	Two-dimensional
3D	Three-dimensional
AHC	Arbitrary 20-degree horizontal correction
AJS-L	Anterior joint space – left
AJS-R	Anterior joint space – right
ANB angle	Angle formed between A point, B point and Nasion point
A-P	Antero-posterior
ANOVA	Analysis of variance
CA-L	Condyle angle – left
CA-R	Condyle angle – right
CR	Centric relation
CO	Centric occlusion
CT	Computed tomography
CBCT	Cone-beam computed tomography
DD	Disc displacement
DICOM	Digital imaging and communications in medicine format file
FA-L	Fossa angle – left
FA-R	Fossa angle – right
FD-L	Fossa depth – left
FD-R	Fossa depth – right
FOV	Field of view
HD	Harvold difference
ICC	Intra-class correlation coefficient
IHC	Individualized horizontal correction
IHVC	Individualized horizontal and vertical correction
LAFH	Lower anterior face height
MDCT	Multi-detector CT

MI	Maximum intercuspation
M-L	Medio-lateral
MPI	Mandibular positioner indicator
MRI	Magnetic resonance imaging
PA	Periapical radiograph
PAN	Panoramic radiograph
PJS-L	Posterior joint space – left
PJS-R	Posterior joint space – right
RBSM	Rigid body spring model
SJS-L	Superior joint space – left
SJS-R	Superior joint space – right
TR	Transcranial radiograph
TMD	Temporomandibular disorders
TMJ	Temporomandibular joint

CHAPTER I

Introduction and Review of the Literature

1.1 Introduction

The sagittal skeletal pattern has been studied over the years as a potential variable in the condyle-fossa position, and therefore a possible risk factor to be considered in the development of TMJ DD (Cohlimia et al, 1996; Vitral et al, 2011; Dalili et al, 2012). Many studies have been conducted to assess whether there is a more consistent condyle-fossa relationship in a given skeletal pattern, which would aid the clinician in identifying patients with a higher risk of developing TMJ DD based on the higher prevalence of a certain condyle-fossa position in a given sagittal relationship of the jaws. The results of these studies are conflicting, and most found that there is no singular condyle-fossa position based on a patient's skeletal pattern (Cohlimia et al, 1996; Vitral & Telles, 2002; Vitral et al, 2004; Katsavrias & Halazonetis, 2005; Rodrigues, Fraga & Vitral, 2009; Rodrigues, Fraga & Vitral, 2009; Krisjane et al, 2009; Vitral et al, 2011; Dalili et al, 2012; Fraga et al, 2013).

A non-concentric position of the TMJ condyle within the glenoid fossa of the temporal bone has been theorized as one of the risk factors for the development of TMJ DD. Many studies were conducted over the past three decades to assess this relationship, achieving conflicting results, and largely unable to find a relationship between condyle position and the presence of TMJ DD (Mongini, 1977; Weinberg, 1979; Brand et al, 1989; Bonilla-Aragon et al, 1999; Pereira & Gaviao, 2004; Sumbulu et al, 2012; Almasan, 2013). Many factors have been implicated in the development of displacement of the temporomandibular joint (TMJ) (Pullinger, Seligman & Gornbein,1993; Laskin, Greene & Hylander, 2006; Okeson 2007; de

Leeuw, 2008; Tanaka et al, 2008, Naeije et al, 2012), and no particular factor is considered as having a more important role in its pathogenesis (Naeije et al, 2012).

According to a comprehensive review of the literature regarding the relationship between skeletal pattern and the TMJ condyle-fossa position conducted by Stamm et al (2004) the current literature falls short in the way the three-dimensional evaluation of the TMJ is being conducted. Those authors found a lack of an unambiguous three-dimensional evaluation of the TMJ condyle position in relation to the glenoid fossa, as most of the studies evaluated by this group of investigators have been assessing the condyle-fossa relationships using a seemingly randomly selected sagittal cut.

Cone-beam computed tomography (CBCT) developed in the early 1990's is an alternative to the low quality images produced by two-dimensional imaging modalities (Scarfe & Farman, 2008). Compared to conventional CT, CBCT technology has the advantage of being considerably lower in cost (Honda et al, 2006) and produces a much lower radiation exposure to the patient (Ludlow, Davies-Ludlow & Brooks, 2003; Schulze et al, 2004; Tsiklakis, Syriopoulos & Stamatakis, 2004). Probably the biggest benefit of this technology is that it has consistently shown equivalent image quality to conventional CT, which will be discussed in more detail in the literature review section (Tsiklakis, Syriopoulos & Stamatakis 2004; Honda et al, 2006; Mishkowski et al, 2007; Honey et al 2007; Hashimoto et al, 2007; Hintze, Wiese & Wenzel, 2007; Suomalainen et al, 2008, Zain-Alabdeen & Alsadhan, 2012). Therefore, the use of CBCT imaging may be a feasible alternative in the evaluation of condyle-fossa relationship of the TMJ.

Thus, the three-dimensional positioning of the condyle in the glenoid fossa in different types of skeletal patterns continues to be undetermined in the current literature. It appears to be of clinical value to use CBCT technology to conduct a three-dimensional assessment of the condyle-fossa relationship in different types of skeletal patterns to assess whether there is a particular condyle-fossa relationship in the different skeletal patterns studied. This assessment is especially valuable considering it can provide a tool that could override the limitations of previous assessments using 2D methods in the study of the position of the hard tissue components of the TMJ.

1.2 Review of the Literature

1.2.1 Anatomy of the temporomandibular joint. The temporomandibular joint (TMJ) is located bilaterally in the cranium, the proximal portion formed by the glenoid fossa located at the squamous segment of the temporal bone of the skull, and the distal portion formed by the condylar process of the mandibular bone. This joint is considered one of the most complex articulations in the human body (Laskin, Greene & Hylander, 2006; Norton, 2007; De Leeuw, 2008).

The portion of the condylar process of the mandibular bone that articulates with the temporal bone of the skull is the condylar head, or also called the condyle. In the coronal view, the condyle has medial and lateral extremities or poles, the medial usually larger than the lateral; it also has a slight convex shape. In the sagittal view the condyle has a pronounced convex shape, and the posterior portion is larger than the anterior (Okeson, 2008).

The portion of the squamous part of the temporal bone that articulates with the condyle is called the articular fossa or glenoid fossa. The fossa is a depression of variable depth where the condyle seats when at rest; it has as a posterior boundary the squamotympanic fissure, and anteriorly a thick convex prominence of variable inclination called the articular eminence (Okeson, 2008).

The TMJ disc is located in between the condyle and the glenoid fossa. It is secured anteriorly by the joint capsule and mediolaterally by collateral ligaments. Posteriorly it presents an area called the bilaminar zone or retrodiscal area, which is heavily vascularized and innervated and that blends into the joint capsule (Laskin, Greene & Hylander, 2006; Norton, 2007; De Leeuw, 2008; Okeson, 2008).

1.2.2 The relationship between the position of the TMJ condyle and sagittal skeletal patterns. Okeson (2008) explains that the TMJ has a "musculoskeletally stable" position, which encompasses the articular disc being located in between the two TMJ bony surfaces, with the condyle positioned superior-anteriorly within the glenoid fossa, which needs to be supported by stable intercuspation of the teeth. When a factor, or a combination of factors, causes a disturbance in the equilibrium between teeth and the TMJ "orthopedic instability" of the system occurs. If one minor disturbance occurs in the absence of additional factors it may lead to insignificant TMJ derangement, however if the disturbance is large, or accompanied by aggravating factors the chances of a large derangement occurring is greater. For example, in a situation of occlusal problems such as cross-bites, open-bites, which are common to many malocclusions/skeletal patterns, the "musculoskeletally stable" position of the condyles needs to be compromised in order

to allow for maximum contact of teeth during function. This scenario could be only minor and cause no major symptoms, but in a patient with aggravating factors such as parafunctional habits, female gender, anxiety/depression, etc, the chances of developing TMD increase exponentially.

Some studies found a relationship between skeletal pattern and a particular condyle-fossa relationship (Seren et al, 1994; Cohlimia, 1996; Katsavrias & Halazonetis, 2005), whereas others did not (Rodrigues, Fraga & Vitral, 2009; Krisjane et al, 2009; Vitral et al, 2011; Fraga et al, 2013). It may be questioned why the correlation between skeletal pattern and the condyle-fossa position would be clinically significant. The answer for that lies on the fact that the condyle position has been linked to the presence of TMJ DD in the literature (Weinberg, 1979; Mongini, 1977; Mongini, 1981; Brand et al, 1989; Brand et al, 1989; Bonilla-Aragon et al, 1999; Pereira & Gaviao, 2004, Almasan et al, 2013), hence, if there is a particular condyle positioning within the glenoid fossa in patients with TMJ DD and this position is also common in a certain skeletal pattern, would the skeletal pattern perhaps act as the primary risk factor for the development of TMJ DD? Although some authors have been trying to answer this question in one way or another (Seren et al, 1994; Cohlimia, 1996; Katsavrias & Halazonetis, 2005, Rodrigues, Fraga & Vitral, 2009; Krisjane et al, 2009; Vitral et al, 2011), this hypothesis has not yet been tested with the use of a valuable 3D analysis. It is also important to add that this is an area of interest for many researchers as studies on this matter have been continuously being published in high impact journals over the years.

Seren et al (1994) conducted a prospective study to evaluate the condyle-fossa relationship of 21 class III malocclusion subjects compared to 18 subjects with normal occlusion using CT. The results evidenced statistically significant differences for the class III group as follows: greater M-L distances of the condyles; smaller A-P dimensions of the glenoid fossa; smaller anterior joint spaces; and significant tendency of protrusive positioning of the TMJ condyle. Cohlimia et al (1996) conducted an evaluation of the morphological condyle-fossa relationship in different malocclusions and skeletal relationships. They evaluated corrected TMJ tomograms of 232 subjects that were categorized dentally based on their Angle classification of malocclusion, and skeletally based on their ANB angle on cephalometric radiography. Their results showed that dental and skeletal class III subjects showed condyles significantly more anteriorly positioned. The dental and skeletal class I and class II groups, however, showed more frequently non-concentricity of condyle-fossa relationship, with no particular direction statistically more common.

Katsavrias & Halazonetis (2005) conducted a retrospective study to evaluate the condyle and fossa shape in class II and class III skeletal patterns. The sample involved images from right and left TMJ tomograms taken from 189 subjects. The sample was categorized in three different groups: class II division 1 (n = 109), class II division 2 (n =47), and class III (n = 33). TMD patients were excluded. The authors were able to conclude that the condylar shape of the class III group was more elongated and inclined anteriorly compared to both class II groups; the fossa shape of the class III group was wider and shallower than the class II groups; the condyle was more anteriorly positioned in the class II div 1 group; the condyle was more

posteriorly positioned in the class II div 2 group; in the class III group the condyle was located more superiorly and in a more centric position A-P than the class II groups. These results evidenced different condyle positions in the different malocclusion groups studied.

Vitral & Telles (2002) conducted a study using axial slice computed tomography imaging to assess the asymmetry between the TMJ condyles in patients with class II division 1 subdivision malocclusion. 30 subjects were evaluated, symptoms of TMD were not considered in their sample selection. The results found no statistically significant differences in condyle symmetry both A-P and M-L. Vitral et al (2004) then published a subsequent article to present the computed tomography evaluation of condyle-fossa relationship of the 30 subjects with class II division 1 subdivision studied in the article discussed previously. The results of this study found no statistical differences between the sides for condyle-fossa relationship, fossa depth and angulation of the posterior wall of the articular tubercle. In terms of individual condyle-fossa relationships, the results found non-concentricity for both sides, where the condyles demonstrated a statistically significant more anterior position; the authors however did not specify if these differences were clinically significant.

Rodrigues, Fraga & Vitral (2009) published another paper on the evaluation of the difference in the condyle-fossa relationships and condylar symmetry. They studied 30 subjects with class II division I malocclusion and 16 subjects with class III malocclusion using CT technology. The results showed for the class II division 1 group a statistically significant difference in the position of the right and left condyles in relation to the mid-sagittal plane. The posterior articular space also showed a

statistically significant difference between the right and left sides for that group. There were no statistically significant right/left asymmetries for the class III group. The condyle-fossa relationship was bilaterally non-concentric for both groups studied, and did not seem to favor any direction in particular.

Rodrigues, Fraga & Vitral (2009) continued their studies on three-dimensional CT assessment of condyle fossa relationship and condylar symmetry. They evaluated a group of 30 class I malocclusion patients. Their results showed a statistically significant asymmetry, with a higher mean for posterior articular space on the right side. The condyle-fossa relationship was bilaterally non-concentric and did not seem to favor any direction in particular, similarly to what was detected for the class II division 1 and class III malocclusion group previously studied by this group of researchers.

Vitral et al (2011) published another paper on the three-dimensional CT assessment of condyle fossa relationship and condylar symmetry. They analyzed normal occlusion patients. A sample of 30 subjects with normal occlusion was selected. Their results showed that there was no particular condyle-fossa relationship in normal subjects. The condyle-fossa relationship was non-concentric bilaterally, and did not seem to favor a direction in particular, as found for class I, class II division 1, and class III malocclusion subjects in earlier publications by this group of investigators. Very recently these authors presented a paper on the final results of their research (Fraga et al, 2013). They concluded that although there was no particular condylar position in patients with normal and abnormal occlusions, it was possible to statistically identify that the class II group produced more non-centralized

condyles, and the normal occlusion group produced the least non-centralized condyles.

Krisjane et al (2009) conducted a study to evaluate the TMJ anatomical differences in class II and class III patients using 3D computed tomography (CT). Their sample included patients with severe sagittal discrepancies that were planned for a combined orthodontic and surgical treatment approach. 15 patients were included in the class II group and 14 patients in the class III group. The results showed that no outstanding differences in condyle size were noted for the groups studied; in both groups there is a tendency for more anteriorly positioned condyles.

Stamm et al (2004) conducted a comprehensive literature review on the three-dimensional (3D) position of the temporomandibular joint at rest. They studied articles from 1899-2011 and found 1903 articles on this topic. Due to a widely variable methodology they ultimately selected 49 studies. The authors' major findings were that the most frequently found methodology for condyle-fossa position was the analytic assessment in a two-dimensional (2D) projection of a sagittal plane elected subjectively, even though many of those studies used 3D data. They claimed that the actual physiological 3D condyle-fossa position was not being established in those studied due to a simplification to a 2D projection, which is a debatable methodological choice in their opinion. They found that the studies with the highest methodological quality described no particular condyle-fossa position; on the other hand the studies with poorer methodological quality were inclined to support a centric position. Finally, the authors concluded that at the time of their publication there was

no unambiguous indication of the actual 3D physiological condyle-fossa relationship available in the literature.

The literature on the topic of the condylar positioning within the glenoid fossa and its relationship with sagittal facial skeletal patterns during the past three decades presents contradicting results (Seren et al, 1994; Cohlimia, 1996; Katsavrias & Halazonetis, 2005, Rodrigues, Fraga & Vitral, 2009; Krisjane et al, 2009; Vitral et al, 2011; Fraga et al, 2013). Even with the advent of advanced imaging techniques such as CT technology the results presented remain conflicting, and the true picture of whether or not there is something unique about the condyle-fossa position in different skeletal patterns remains obscure (Rodrigues, Fraga & Vitral, 2009; Krisjane et al, 2009; Vitral et al, 2011; Fraga et al, 2013). As pointed out by Stamm et al (2004) it can largely be due to the use of a 2D analysis, even when a 3D imaging modality is used, but it can very well be a combination of methodological issues, including imaging modality, imaging reconstruction error, or investigator error. Other possibilities may lie on the study design; the way the sample selection was carried out could largely affect the results, in both inclusion and exclusion criteria matters. For example, how the skeletal pattern was standardized, as only dental, only skeletal, or both, or which cephalometric value was used to select the patients on the basis of their sagittal skeletal relationships can be critical factors. Issues in the selection of those variables may lead to results that may not properly answer the question that the literature on this topic has been trying to answer. Perhaps more stringent inclusion criteria in terms of skeletal and dental classification, as well as the use of an analysis more closely to a 3D analysis as possible, could draw more truthful results. This way

a more reliable interpretation of the results could be accomplished on whether or not there is a more common positioning of the TMJ condyle within the glenoid fossa in patients that present a certain antero-posterior relationship of their jaw bony components.

1.2.3 Temporomandibular joint disc derangement disorder. TMJ disc derangement is only one group of disorders described under the umbrella of temporomandibular disorders (TMD). It has been estimated that approximately 40% to 75% of the general population will experience signs of TMD's at one point in their lives, but 3.6% to 7%, require intervention (de Leeuw, 2008). There are two main types of disorders in the positioning of the TMJ disc: disc displacement with reduction and disc displacement without reduction. The first develops from the disc displaced anteriorly in closed mouth position, and when mouth opening occurs, the disc is pulled upwards to a superior position in relation to the condyle; this mechanism typically creates a noise called clicking or popping. The latter occurs also from the disc displaced anteriorly in closed mouth position, but when mouth opening occurs the disc does not move superiorly to the top of the condylar process, this form of disc derangement is referred as "closed lock" of the jaw and typically there are no joint noises present (De Leeuw, 2008; Okeson, 2008).

Numerous risk factors have been proposed in the development of displacement of the temporomandibular joint (TMJ) disc, such as occlusal variables (Pullinger, Seligman & Gornbein,1993; Okeson 2007; de Leeuw, 2008), trauma (Laskin, Greene & Hylander, 2006), parafunctional habits (Tanaka et al, 2008), and TMJ condyle-fossa position (Mongini, 1977; Weinberg, 1979; Brand et al, 1989;

Bonilla-Aragon et al, 1999; Pereira & Gaviao, 2004; Sumbulu et al, 2012; Almasan, 2013). Unfortunately the results of the reports of etiological factors in relation to TMJ DD in the current literature are very diverse, and the appropriate understanding of the factors involved in the development of the TMJ disc displacement (DD) disorder remains obscure (Naeije et al, 2012), particularly because most studies on this topic use a two-dimensional methodology for condyle-fossa evaluation (Stamm et al, 2004).

A recent study conducted by Ikeda and Kawamura (2013) using CBCT technology to assess condyle position in patients previously diagnosed with DD with the use of MRI. Their results found that DD was statistically significantly related with a more posterior and superior condylar position depending on the extent of disc displacement. The authors concluded that dislocation of the articular disc could modify the position of the TMJ condyle leading to changes in the size of the joint compartments. It was however not clear if the changes in condyle position were related to the cause or a consequence of TMJ DD.

TMJ disc derangement has been considered as risk factor in the development of degenerative disease of the TMJ (TMJ osteoarthritis – OA) according to the guidelines for diagnosis of orofacial pain published by De Leeuw (2008). These guidelines classify TMJ DD among those in relation with the development of secondary OA. Boeddinghaus & Whyte (2013) explained that remodeling of bone and osteoarthritis may follow the dislocation of the TMJ disc.

The use of CT technology in the assessment of bony and disc changes is considered by Boeddinghaus & Whyte (2013) as a great imaging choice to aid in the

diagnosis of a large range of TMJ pathologies, including TMJ internal disc derangement and osteoarthritis. They describe that CT is the modality of choice in situations of trauma and primary bone lesions (such as osteoarthritis), and consider that it can be satisfactorily used as a substitute to MRI for other TMJ conditions, when the use of this imaging modality is not possible due to availability, pre-existing conditions, etc.

They listed disc displacement, degenerative changes, fractures, tumors and ankylosis as some of those pathologies. Internal disc derangement signs can be identified in CT images by decrease in joint compartments, disc deformities and erosions. The features of osteoarthritis seen in the CT images may include diminishing of the joint spaces, remodeling and flattening of the articular surfaces (including glenoid fossa, articular eminence and condylar head), sclerosis and thickening of the cortical bony layer, and in more severe cases subcortical cysts and ostephytes.

1.2.4 The relationship between the position of the TMJ condyle and the presence of temporomandibular disorders. Throughout the past 4 decades several published studies assessed the TMJ condyle-fossa relationship as it has been hypothesized it could be a risk factor for the development of temporomandibular disorders, particularly TMJ DD (Mongini 1977; Weinberg, 1979; Mongini, 1981; Brand et al, 1989; Alexander, Moore & Dubois, 1993; Bonilla-Aragon et al, 1999; Pereira & Gaviao, 2004; Dalili et al, 2012). Those studies achieved contradicting results in the most part, as described in more detail below.

Weinberg (1979) stated that there was a difficulty in the treatment of TMJ dysfunction due to a deficient understanding of its multifactorial nature. He assessed the condyle-fossa position in 55 patients suffering from acute TMJ dysfunction in comparison with 61 subjects without TMJ issues using what the author calls "TMJ radiographs". The author found condylar retrusion in 71% of the acute TMJ dysfunction group, compared to 36% found in the control group. He concluded that the high incidence of condylar retroposition in the TMJ dysfunction group is a clinically significant factor in the etiology of that type of dysfunction. Mongini (1977), found condyle displacement from a centric position in 51.4% of the patients studied. He used tomograms of the TMJ to evaluate the condyle-fossa relationship of 70 subjects with TMD symptoms without a control group. It is worth noting that nearly half of those subjects presented concentric condyles even though those patients presented an internal articular derangement disorder.

In the early 1980's Mongini (1981) published another paper on the topic. This time he evaluated the condyle position of 30 patients clinically diagnosed with TMD. Both transcranial radiograph (TR) and tomograms were taken for each patient. The condyle was considered centered based on the uniformity of the articular space; differences of more than 1mm in the anterior or posterior direction would describe the condyle as displaced. Using TR the condyles were posteriorly displaced in the large majority of the patients studied (27 patients), which was corroborated by serial tomograms.

Brand et al (1989), on the other hand, found the presence of condyle retroposition did not seem to correlate well as a predictor for internal derangement of

the TMJ. They conducted an evaluation of the condyle-fossa relationship and the presence of TMJ disc displacement in order to determine if the condyle position could be used as a predictor for the presence of abnormal positioning of the TMJ articular disc. They evaluated 243 patients, and used arthrograms to assess internal derangement and tomograms to evaluate condyle-fossa relationship. Their results showed that the majority of the sample presented with TMJ internal derangement (211 patients). In the TMD group, 64% to 73% had retropositioned condyles, but 41% to 53% of the joints studied that were considered free of internal derangement (32 patients) were also found to have condylar retroposition. Their results support the view that posteriorly positioned condyles are also fairly common in TMD-free subjects.

Alexander, Moore & Dubois (1993) evaluated the condyle-disc-fossa relationship comparing articulator mountings and MRI imaging. Their sample consisted of 23 adult males, without TMD symptoms, and with a class I molar relationship. Their methods consisted in recording the bite in CO (maximum intercuspation), CR (positioning the condyles more superiorly on the posterior slope of the glenoid fossa eminence) with the aid of the mandibular position indicator (MPI), an instrument that compares the position of the maxilla in relation to the mandible in the 3 planes of space. They also recorded the mandible in retruded position by manipulating the mandible to its most retruded position. An acrylic positioner was fabricated for the three bite records and a MRI was taken for each subject using the three different bite positioners. Two independent examiners defined the concentricity in a subjective manner as they evaluated the condylar position

without making measurements and describing its position as retruded, concentric and protruded. Their results showed that approximately half of the sample did not demonstrate a concentric condyle-fossa relationship. Approximately half of the sample maintained their condyle-fossa relationship for CR, CO and retruded position. These authors concluded that diagnosis of TMJ health based on a concentric condyle-fossa relationship was not supported by their study.

Braun (1996) evaluated the TMJ condyle-fossa relationships using standard sagittal cephalometric radiographs of 38 TMJ symptom-free volunteers. 89% of the TMD-free sample studied showed a non-concentric position of the condyle within the fossa. The author stated that concentricity of the TMJ condyle by itself might very likely not be a compelling factor in the diagnosis of TMD. Dalili et al (2012) found a completely different result in their evaluation of the position of the condyle in 40 subjects with a class I skeletal pattern and no history of TMD. They used CBCT technology as their imaging modality and defined concentricity as having the anterior and posterior joint spaces equal or nearly equal. Their results found a centric condyle position in 92.5% of their TMD-free sample.

Bonilla-Aragon et al (1999) assessed the position of the condyle as a predictor of the presence or absence of TMJ disk displacement. Their sample included 52 TMD asymptomatic patients and 130 patients with symptoms of TMD. The main TMD symptom was joint pain with or without pain on movement, limited range of mouth opening, and joint noises. The imaging modality used for the assessment of TMJ disk displacement was MRI. The joint measurements were made using tomograms. The authors concluded that the condyles of the symptomatic group were significantly

more posteriorly positioned than the controls (41.3%). The condyle-fossa relationship was found, however, to be a poor predictor for the presence of TMJ DD as posteriorly displaced condyles were found in 23.1% of the sample of TMD-free subjects.

The study conducted by Pereira & Gaviao (2004) explored the matter of TMJ condyle-fossa position and the presence of temporomandibular disorders further. They also failed to find a direct relationship between the presence of TMD and the position of the TMJ condyle within the glenoid fossa. Corrected linear tomograms of 20 patients diagnosed with TMD and 20 patients with no TMD as the control group were studied. Their results evidenced a statistically significant higher number of posteriorly positioned condyles in the TMD group. There was, however, a large diversity in condyle position for both the groups studied.

Ikeda & Kawamura (2009) assessed the optimal condyle position in the glenoid fossa of normal joints using sagittal CBCT images. They used a sample of 22 subjects with no signs and symptoms of TMD. Their results found a small variability in condyle-fossa position, with the condyle more anteriorly positioned. In 2011 Ikeda and Kawamura published a follow-up to their 2009 paper, this time they presented the assessment of optimal condylar position on the coronal and axial views using the same sample of asymptomatic patients, and again found a small variability in condyle-fossa position, with a more anteriorly positioned condyle.

Almasan et al (2013) conducted a MRI study of TMJ disk and joint variations on the coronal and sagittal view in a sample of 37 TMD patients (74 joints), without a control group. Their results found that in the sagittal view the condyles were posteriorly positioned in 62.7% of the joints with disc displacement. There was a

statistically significant difference of the superior and posterior joint space between normal disc position and disc displacement with reduction. In the coronal view there was a significant increase in the distance of the most medial condyle point to the midline in joints with disc displacement. The results of this study imply that the presence of disc displacement induces changes in condyle-fossa position in both the sagittal and coronal planes.

A recent paper published by Kandasamy, Boeddinghaus & Kruger (2013) used MRI technology to investigate whether there is a difference in the condyle position of the same subject under 3 different bite registrations – centric occlusion, centric relation and Roth power centric relation. They investigated 19 TMD-free subjects with non-specified positive overbite and overjet. The MRI measurements used the poles of the condyles and the deepest concavities of the glenoid fossa to measure the articular spaces, the authors however did not specify if those measurements were performed in a 3D manner. Their results showed that 87% of the condyles studied showed a concentric position within the glenoid fossa, and that there were no statistically significant differences in condyle position in the 3 bite registrations studied. These findings support the conclusion that bite manipulations do not significantly change the condyle position; therefore its use as a preventive or a therapeutic measure for TMD is likely non-beneficial.

Based on the studies discussed, it is possible to conclude that although the posterior position of the condyle was a common finding in subjects with TMD in all the studies discussed (Weinberg, 1979; Mongini, 1977; Mongini, 1981; Brand et al, 1989; Brand et al, 1989; Bonilla-Aragon et al, 1999; Pereira & Gaviao, 2004,

Almasan et al,2013), it was also found in TMD-free patients in a considerable frequency (Brand et al, 1989; Alexander, Moore & Dubois, 1993; Braun, 1996; Bonilla-Aragon et al, 1999; Pereira & Gaviao, 2004; Dalili et al, 2012) that varied from 7.5% (Dalili et al, 2012) to 89% (Braun, 1996). The lack of agreement on whether or not there is a cause-effect relationship between the presence of TMJ DD and a particular position of the TMJ condyle within the glenoid fossa cannot yet be seen as a matter of no clinical or anatomical relevance, considering that the large majority of the studies in the literature have been using 2D technology in their analysis or conducting 2D analysis using 3D imaging. It is the objective of the present study to conduct a 3D analysis of the TMJ using CBCT in the closest fashion to a 3D analysis possible, considering that a true 3D investigation of the TMJ is not yet available for this type of technology. The development and improvement of 3D analysis as the gold standard for the radiographic evaluation of the relationship of the TMJ structures will allow for a better judgment and scrutiny to the previous results of condyle-fossa position in the literature.

1.2.5 Cone-beam computed tomography technology. The interest in developing CBCT technology to the dental field initially happened in 1995 in Italy, with the construction of the first CBCT system for the maxillofacial region that became marketed specifically for dentists, the NewTom 9000. The initial big advantages of CBCT imaging was that it could provide an alternative to conventional CT by using a reasonably less costly radiation detector, using less physical space, and particularly exposing the patient to less radiation (Angelopoulos, Scarfe & Farman, 2012).

CBCT technology is able to acquire images in a different manner in comparison to conventional CT scanners. The difference lies primarily on the fact that instead of using a fixed gantry like in conventional CT, it uses a rotating support (where an x-ray source and detector is located) in the acquisition of the images (Mozzo et al, 1998; Scarfe & Farman, 2008).

Conventional CT uses a fan-shaped x-ray beam in a helical progression, whereas CBCT technology uses a source of ionizing radiation with the appearance of a cone directed to the middle of the area of choice with the x-ray source revolving 360 degrees. These rotations are able to obtain a series of exposures of approximately one for each degree, which enables the acquisition of data with only one rotational sequence of the scaffold, decreasing the time of the procedure and the radiation exposure. This also decreases the time consumed in imaging reconstruction, as the data slices acquired by CBCT can be effectively used for subsequent image reconstruction as one stack of images (Mozzo et al, 1998; Scarfe & Farman, 2008).

In conventional CT the use of a helical progression acquires images in individual slices, which are only later connected to each other to form a 3D image, this lengthens the process of acquisition of the final image because each of those slices requires an individual 2D reconstruction (Mozzo et al, 1998; Scarfe & Farman, 2008).

Another important factor is that the images acquired by CBCT enable visualization in all 3 planes of space (axial, coronal and sagittal), as well as in a panoramic view. These images also have the further advantage of not suffering from magnification or distortion in both size and shape (Parks, 2000; Danforth, Dus &

Mah, 2003). Which is a particularly valuable characteristic as it enables a reliable evaluation of the anatomical structures, both in terms of anatomical contours and measurement of distances and angles.

A recent literature review conducted by Angelopoulos, Scarfe and Farman (2012) explained a very important difference between conventional CT and CBCT imaging in terms of spatial resolution, which allows the investigator to differentiate fine contours of anatomical structures in close relationship. CBCT produces images that are equal in the three planes of space (x, y and z), which is described as an "isotropic" voxel resolution. Conventional CT imaging, on the other hand, produces images called "anisotropic" as the resolution in the z axis is significantly lower than in the x and y axis. This allows for a better resolution of the axial plane in comparison to the coronal and sagittal planes, as those are drawn from the longitudinal reconstructions involving the z-axis.

The importance of slice thickness in conventional CT technology is in close relationship with spatial resolution, as the drawback of "anisotropy" described above can only be minimized when the slice thickness is of approximately 0.40mm or less. In imaging reconstructions with 1mm slice thickness it is quite obvious that the spatial resolution in the coronal and sagittal view will be diminished. Most CT scanners nowadays use a slice thickness of 0.5mm or 0.625mm in order to achieve a near-isotropy of the voxel resolution (Angelopoulos, Scarfe and Farman, 2004).

The matter of radiation exposure has been an early point of discussion in relation to the use of CBCT technology. Ludlow et al (2003) studied the effective radiation dose used by different CBCT units. Their results found the effective

radiation dose of the machines studied to be between 2% and 23% of that encountered for conventional CT scanners. Conversely, the CBCT radiation dose may be several to many times greater of that found for a single panoramic 2D image. The results published by this group of authors are in close agreement with those found by Schulze et al (2004). These authors found that the radiation effective doses of CBCT systems to be considerably less than conventional CT and greatly higher than conventional radiography.

The ADA, 2012 position paper on CBCT presented the radiation effective dose estimates for common dental radiographs and CBCT, based on the work of Ludlow et al (2008), Pauwels et al (2012), and the SEDENTEXTCT project (2011) guidelines. According to the estimates presented it is possible to infer that, depending on the field of view (FOV) selected, brand of machine and voxel size determined, the effective dose of CBCT can be similar to that of panoramic radiography or full mouth series if the CBCT FOV and voxel size is adjusted.

Pauwels et al (2012) carried-out a study with the objective of assessing the radiation dose distribution for a range of CBCT units, different field of views (FOVs), and full (360°) or partial (180°) rotations of the beam. Their results found that for the 360° and 180° the radiation dose to the radiosensitive organs increased as the FOV was enlarged. The salivary glands received the most contribution from the effective dose, followed by thyroid, red bone marrow, and the esophagus. Schilling & Geibel et al (2013) determined that the reduction of effective doses could be accomplished in two main manners: choosing lower resolutions and mAs settings, and selecting

smaller FOVs. They explained that the selection of the small FOV is particularly important as it avoids exposing radiosensitive organs.

The matter of accuracy of the CBCT images in comparison to conventional CT has been studied extensively. Honda et al (2006) compared the reliability of the diagnostic information provided by CBCT images in comparison to helical CT for the detection of osseous abnormalities of the mandibular condyle. They used 21 mandibles from autopsy specimens for their study, and the direct macroscopic evaluation was their gold standard. The authors found no significant differences between the results given by CBCT and CT technology, and therefore describe CBCT as a lower dose and lower cost alternative to conventional CT in the diagnosis of condyle osseous abnormalities. Michkowski et al (2007) studied the accuracy in linear distances and volumes provided by CBCT in comparison to multidetector row CT, their results showed the CBCT images provided acceptable information with no relevant differences to CT images.

Barghan, Tetradis & Mallya (2012) carried-out a comprehensive review of the literature on the use CBCT technology for TMJ evaluation. The authors stated based on their review that the CBCT technology offers high resolution multi-slice images with the additional advantage of exposing the patient to less radiation compared to conventional CT. Hence, the authors concluded that CBCT images are able to offer valuable data in the diagnosis of many disorders of the TMJ, such as different types of arthritis, trauma and development disorders. In terms of disc displacement disorders they explain that this type of imaging cannot visualize the disc, but there are alterations that can be detected in CBCT images that can suggest the presence of disc

displacement, such as a more posterior condyle-fossa relationship, and limitation in range of condyle translation.

The value of CBCT technology in the three-dimensional study of the relationships of the maxillofacial structures, such as has been done two-dimensionally for many decades with cephalometric analysis, became a topic of research interest. Lagravere et al (2009) conducted a study to evaluate the intra-rater and inter-rater reliability of three-dimensional selection of traditional cephalometric landmarks. Twenty-four CBCT images were analyzed, the main examiner conducted the landmark selection five times, and four other examiners located the same landmarks once. Their results found acceptable inter and intra-examiner reliability for all landmarks studied.

Gribel et al (2011) conducted a comprehensive study to compare the accuracy and reliability of craniometric measurements using lateral cephalometric radiography (cephs) and CBCT images. They used 25 dry skull models for their analysis, and placed markers on ten known cephalometric landmarks. Each skull was imaged using CBCT and cephalometrics; subsequently one examiner identified the selected landmarks in each type of imaging, for the CBCT using a software module and for the cephalometrics through hand tracing. Their results found no statistically significant difference between the CBCT and the direct craniometric measurements; conversely, there was a statistically significant difference between the cephalometrics and the direct craniometric measurements. The authors concluded that craniometric measurements using the CBCT technology were exceptionally precise and therefore can be used for craniofacial analysis.

Zamora et al (2012) also used CBCT images to assess the reliability of landmarks commonly used in cephalometrics. He evaluated 41 landmarks in the 3 axes. Intra- and inter-reliability was calculated for all axes. Their results showed that the Intra-Class Correlation coefficient (ICC) was very high (equal or higher to 0.99), and the most reliable axis was the z axis. Fuyamada et al (2011) studied the method of three-dimensional analysis with definitions of the landmarks in the three-dimensional axis (x, y, and z) described in the above papers. They aimed to determine if the use of landmark definitions for each plane of space (procedure 2) would be of any added value for 3D analysis of craniofacial landmarks, in comparison of the traditional definitions set for cephalometric landmarks (procedure 1). They found that there were no statistically significant differences between the two procedures. The procedure 2, however, showed better reproducibility and smaller standard deviations.

Periago et al (2008) studied the difference in accuracy of 20 linear measurements using CBCT images in comparison to measurements taken directly from a skull model. They found the differences to be statistically significant, but still very small (1.13%, SD +- 1.47), therefore the accuracy of linear measurements using CBCT images can be considered satisfactorily clinically precise for analysis of the craniofacial structures. Brown et al (2009) studied the linear accuracy of measurements taken from CBCT images, and used a skull model as a gold standard. Their results found that the linear measurements had variable accuracy, which could have been related to variations in the landmark selection, not necessarily distortion in the image itself. Regardless, the linear measurements involving the only TMJ

landmark studied (e.g. condylion or superior-most point of the head of the condyle) did not show statistically significant differences.

Patcas et al (2012) assessed the accuracy of linear intraoral measurements using CBCT and multidetector CT (MDCT), also with a skull model as a gold standard. Their results found that the CBCT showed a mildly increased reliability in the linear measurements in comparison to multidetector CT. Abboud et al (2013) found slightly different results in their study. The medial grade CT was the most accurate, but the measurements of distances for the bony components of the mandible made by the five CBCT machines studied differed only slightly from those made by the medical CT. Nevertheless, they stated that these discrepancies are likely not clinically significant for most diagnostic purposes.

Brown et al (2009) studied the linear accuracy of 16 measurements using different CBCT projections (153, 306, and 612 slice projections). They found that the number of projections did not affect the accuracy of the measurements. Hashem et al (2013) conducted a study using porcine specimens to evaluate the accuracy of measurements using high (360° rotation) and low (180° rotation) resolution CBCT images. Their results found no statistical significant difference between high and low-resolution CBCT images for the distances studied. The results of these two papers show that both high resolution and high number of projections is not needed in order to achieve reasonable accuracy of measurements using CBCT technology. These findings are particularly valuable as they show that useful information can be drawn from CBCT images without the need exposing the patient to added radiation.

1.2.6 Methods for radiographic condyle-fossa position evaluation. Blashke & Blashke (1981) recognized the need for a reproducible assessment of the TMJ condyle-fossa relationship and proposed an evaluation model in the early 1980's, as differences in anterior and posterior joint spaces could be of clinical value in the development of TMD's. Lateral corrected tomograms were used as the imaging of choice. Their model essentially involved the location of the mid-point of the condyle and its connection with 5 different points located in the anterior and posterior fossa, forming a triangle anteriorly and posteriorly. They concluded that this was an effective model to quantitatively evaluate the condyle-fossa relationships, within the same subject over time and between subjects.

In the mid 1980's Pullinger & Hollender (1986) conducted a linear tomogram study to assess the variation in the measurements of condyle-fossa relationship using different methods. The methods presented by this study would later become one of the most used for condyle-fossa assessment in the literature. Seven different methods were studied: subjective method (condyle position assessed by visualization only); quantitative method (area and linear measurements made with the aid of a graphics tablet); linear measurement method of the subjective closest joint space (subjective measurement of the closest posterior and anterior interarticular spaces); quantitative methods that use a protractor matrix (use of a protractor overlay to locate the measurements, 3 different methods using a protractor were studied); quantitative method measuring the horizontal displacement of the condyle midpoint from the fossa midpoint. The method of linear measurement of the subjective closest posterior and anterior articular space was found to be easy to use and to have a high

repeatability. This was also the method that most closely correlated with the subjective scoring with the advantage of demonstrating less inter-observer variation. As a result, the subjective linear measurement was chosen by the authors as the method of choice to evaluate the condyle-fossa relationships radiographically. Pullinger & Hollender (1985) then conducted a subsequent study using five of the methods described above (the subjective method, the 3 protractor overlay methods, and the method of linear measurement of the subjective closest posterior and anterior articular space) to compare the use of transcranial radiographs (TR) and linear tomograms in the assessment of the condyle-fossa relationship. Similarly to their previous study, the subjective closest joint space method was considered the best method, but they stated the use of a skull model as a gold standard is desirable to better support their conclusion.

In the mid 1980's to the 2000's the use of three-dimensional radiographic modalities, such as three-dimensional computed tomography (CT) and magnetic resonance imaging (MRI), became increasingly utilized in studies of TMJ position.

Moadabb et al (1985) described a 3D reconstruction technique using CT technology. The images were reconstructed using software that enabled the visualization of the anatomical structures of the TMJ in the axial, coronal and sagittal view. They describe this method as a great option in the evaluation of joint spaces. The authors concluded that this method could simplify the diagnosis of TMD as it could avoid exploratory invasive procedures. They described cost, radiation exposure and availability of the technology as limiting factors to its routine clinical application. Tyndall et al (1992) also conducted an assessment of the positional changes of the

mandibular condyle position using CT imaging. The landmarks used to assess condyle position included anterior condyle surface, superior condyle surface, medial pole and lateral pole. The authors concluded that CT imaging was very accurate in identifying inferior condylar changes, as detection of lateral and posterior changes were recorded with less accuracy in their study.

The studies conducted a group of researchers from Brazil (Vitral & Telles, 2002; Rodrigues, Fraga & Vitral, 2009; Rodrigues, Fraga & Vitral, 2009; Vitral et al, 2011, Fraga et al, 2013) proposed a methodology for the evaluation of TMJ condyle-fossa relationship. The method for condyle evaluation involved measurements in the axial plane: linear measurement of the largest A-P and M-L distances of the condyle; the angle between the long M-L axis of the condyles and the midsagittal plane; a line drawn from the geometric center of each condyle to the midsagittal plane, then the distance from where the right and left side intersect in the midsagittal plane was recorded. The method for condyle-fossa evaluation involved measurements in the sagittal plane with the patient in MI, as follows: fossa depth (line from most inferior point of articular tubercle to most inferior point of auditory meatus, and measurement from most superior point of fossa to that line); angulation of posterior wall of articular tubercle (angle formed by the plane of the posterior wall of the articular tubercle to the inferior articular tubercle-auditory meatus line); anterior joint space (shortest distance from anterior most point of the condyle to the posterior wall of the articular tubercle); superior joint space (shortest distance from superior most point of the condyle and the superior-most point of the fossa), posterior joint space (shortest distance from posterior-most point n the condyle to the posterior wall of the fossa).

These authors used mainly an axial and sagittal slice to perform their measurements, although a 3D imaging modality was used, a 2D evaluation was carried-out.

Endo et al (2011) also used conventional CT imaging to conduct his study on the condyle and fossa position. They conducted their measurements by selecting one slice in each plane of space for image reconstruction, using a slice thickness of 1mm. The condyle-fossa relationship was studied by using the reconstructed surface images. The paper by Terajima et al (2008) was used as the basis for their methodology. They used the software 3D-Rugle (Medic Engineering) and divided the surface of the condyle in small triangles, then defined the centre of them; thereafter the smallest distance from those points to the glenoid fossa was determined. Although this methodology uses a three-dimensional approach to the analysis of condyle-fossa relationship the use of a 1mm slice thickness introduces error in the image reconstruction.

Costa et al (2008) presented a 3D imaging study of the TMJ using MRI technology, with the aim of determining the value of this method in the diagnosis of TMJ DD. They evaluated 42 subjects previously clinically and radiographically (MRI images) diagnosed with TMJ DD and 18 TMD-free subjects. The software MRICro® was used to convert the MRI images to the ANALYZE® format. The software ITK-SNAP® was used to study the 3D reconstructed images, which allowed for manual segmentation of the images, and the use of different colors for the fossa, articular disc and condyle to facilitated the analysis. This software also allowed the visualization of those structures on random planes. The patients were evaluated in open and closed mouth position. As MRI technology allows for a clear visualization of soft tissue

structures, the patients were evaluated for the position of the TMJ disc in three categories: normal, disc displacement with reduction, and disc displacement without reduction. The authors found that their proposed 3D technique on the diagnosis of DD showed an excellent correlation with MRI findings.

In the late 2000's and early 2010's studies assessing the TMJ condyle-fossa position started to use CBCT as the imaging method of choice. Ikeda & Kawamura (2009) assessed condyle position using CBCT images. The sagittal slice selected for the analysis was acquired by finding the long axis of the condyle and bisecting a vertical plane, therefore although a 3D imaging system was used a 2D analysis was performed for this study. The authors report the intra-reliability differences found were smaller than 0.08mm. Sumbulu et al (2012) also used CBCT imaging to. The image measurements were accomplished on the central sagittal slice of the TMJ; even though a 3D image was used a 2D analysis was carried out.

Based on the analysis of the literature accomplished presently, it is possible to corroborate with Stamm et al (2004)'s conclusions in the mid 2000's. The present review of both the early and the most recently published literature on the theme of TMJ condyle-fossa relationship evaluation showed that the studies evaluated continue to lack in the aspect of conducting a three-dimensional analysis of patients with different sagittal skeletal relationships. The literature on this topic also lacks in determining whether or not skeletal pattern plays a statistically significant role in the way the TMJ condyle is positioned in relation to the articular fossa.

1.3 Purpose of the Study

1. Construct a three-dimensional methodology to analyze the condyle-fossa relationship using CBCT technology, with the following objectives:

1.1 Construct an analysis that can be easily applied in future research, and particularly by the clinician and support staff in private practice;

1.2 Select anatomical landmarks on the TMJ condyle and glenoid fossa that can appropriately assess the relationship between these two joint structures;

1.3 Analyze the reproducibility and reliability of the landmarks chosen by using intra and inter-reliability tests;

1.4 Create linear and angular measurements between the selected anatomical landmarks to appropriately assess the angle of the joint structures (i.e. whether the condyle and fossa surfaces presented a flatter or rounder surface), as well as the relationship between the TMJ condyle and glenoid fossa. This includes: angle of the condyle; angle of the glenoid fossa; depth of the glenoid fossa; and anterior, superior and posterior joint spaces;

2. Determine and compare the three-dimensional position of the TMJ condyle in relation to the glenoid fossa in class I, class II and class III skeletal patterns and statistically determine whether the differences are significant or not;

3. Compare the sagittal angle of the TMJ condyle in class I, class II and class III skeletal patterns and statistically determine whether the differences are significant or not;

4. Compare the sagittal angle of the TMJ glenoid fossa in class I, class II and class III skeletal patterns and statistically determine whether the differences are significant or not.

5. Compare the depth of the TMJ glenoid fossa in class I, class II and class III skeletal patterns and statistically determine whether the differences are significant or not.

1.4 Thesis Statement

Null Hypothesis #1: The three-dimensional method for three-dimensional evaluation of TMJ condyle-fossa position proposed is not statistically sufficiently reproducible and reliable.

Null Hypothesis #2: There is no statistically significant difference in the three-dimensional position of the TMJ condyle in relation to the glenoid fossa in different types of skeletal patterns.

Null Hypothesis #3: There is no statistically significant difference in the angle of the TMJ condyle in different types of skeletal patterns.

Null Hypothesis #4: There is no statistically significant difference in the angle of the TMJ glenoid fossa in different types of skeletal patterns.

Null Hypothesis #5: There is no statistically significant difference in the depth of the TMJ glenoid fossa in different types of skeletal patterns.

Chapter II

Subjects and Methods

2.1 Sample Selection

This research project used cone-beam computed tomography (CBCT) images in order to retrospectively analyze the three-dimensional (3D) position of the temporomandibular joint (TMJ) condyle in different types of skeletal patterns (malocclusions).

CBCT images were obtained from a database at the University of Alberta Graduate Orthodontic Program (Edmonton, Alberta, Canada). Three experienced dental assistants trained and calibrated equally took the images. These images were taken as part of a standard record for orthodontic diagnosis and treatment planning. Consent for the use of these patients' records has been authorized for future research use. Appropriate ethics approvals were acquired from the University of Alberta Ethics Research Board and University of Manitoba Ethics Research Board.

The sample was consecutively selected and included both males and females in their full permanent dentition (second molars were not necessarily present). This included patients from age 11 and older. Thirty patients were selected for each malocclusion group, with a total of 90 patients.

The exclusion criteria included:

- ✓ Patients with a history of TMJ dysfunction, including joint noises, joint pain, jaw locks, mouth opening limitation (assessed through retrospective chart review)
- ✓ Patients with a history of jaw surgery (rigid internal fixation present on radiographs)
- ✓ Patients with skeletal asymmetries (visually obvious on intra and extra-oral photos)

- ✓ Patients with open-bites (1mm or larger on intra-oral photos)
- ✓ Syndromic patients (visually detected on intra and extra-oral photos)

In order to select the sample on the basis of skeletal pattern, a preliminary search was carried out within the database of patients that had a CBCT scan taken as part of their pre-treatment records. The skeletal pattern was classified as:

- ✓ Skeletal class I
- ✓ Skeletal class II
- ✓ Skeletal class III

The skeletal classification was assessed on the basis of two-dimensional cephalometric parameters. The cephalometric measurements used included the ANB angle, Wits appraisal, and Harvold difference. The skeletal relationship was determined based on the agreement of 2 or more cephalometric measurements (Table 1). The cephalometric values were assessed retrospectively using the University of Alberta Graduate Orthodontic Program patient database. The digital cephalometric tracings were accomplished using Dolphin® software (Patterson Technology, Chatsworth, CA, USA) and carried out by the orthodontic resident assigned to each patient, and approved by the orthodontic clinical instructor assigned to the case.

Table 1 Cephalometric skeletal pattern classification

	Class I	Class II	Class III
ANB	0° ≤ ANB ≥ 4°	ANB > 4°	ANB < 0°
Wits	Females: 0° ≤ Wits ≥ 1°	Females: Wits > 1°	Females: Wits > 0°
	Males: -1° ≤ Wits ≥ 0°	Males: Wits < 0°	Males: Wits < -1°
Harvold difference (HD)	9 to 11 years old: 16mm ≤ HD ≥ 24mm	9 to 11 years old: HD < 16mm	9 to 11 years old: HD > 24mm
	12 to13 years old: 19mm ≤ HD ≥ 27mm	12 to14 years old: HD < 19mm	12 to14 years old: HD > 27mm
	14 years old and older: 22mm ≤ HD ≥ 30mm	14 years old and older: HD < 22mm	14 years old and older: HD > 30mm

Athanasiou (1995); Proffit et al (2007)

The dental classification was assessed for skeletal class II group only on the basis of molar relationship and overjet, through the evaluation of intra-oral photos. The skeletal class II group included only patients with unilateral or bilateral Angle class II molar relationship (class II 1/4 cusp or larger) associated with an increased overjet (Bjork III overjet cephalometric measurement of 4mm or larger). This process excluded class II skeletal patients with a class II division 2 dental malocclusion.

Once the images were selected and appropriately categorized, each cone-beam scan was analyzed in regards to the TMJ position by the primary investigator (I.G.). A total of 180 joints (90 subjects/CBCT scans) were evaluated.

The sample size was chosen on the basis of the literature review on the topic of three-dimensional evaluation of the temporomandibular joint using three-dimensional imaging techniques (e.g. MRI, medial grade CT, CBCT) conducted previously (Tyndall et al, 1992; Alexander, Moore & Dubois, 1993; Seren et al 1994; Vitral & Telles, 2002; Vitral et al, 2004; Menezes et al, 2008; Rodrigues, Fraga & Vitral, 2009; Rodrigues, Fraga & Vitral, 2009; Vitral et al, 2011; Endo et al, 2011; Ikeda & Kawamura, 2009; Almasan et al, 2013; Sumbulu et al, 2012; Dalili et al, 2012). The use of 90 patients (30 patients divided in 3 groups) by the current study appears as an appropriate option considering it is equal or larger to all studies referenced above, all those studies were published in high-impact journals. The only exception is the study conducted by Bonilla-Aragon et al (1999) that used a larger sample of 52 TMD asymptomatic patients and 130 patients with symptoms of TMD. This study's purpose, however, was an evaluation of condyle position in a sample of TMD/TMD-free subjects, not an assessment of condyle-fossa position in different skeletal patterns, which is the purpose of the current study. Additionally Bonilla-Aragon et al (1999) used MRI imaging and not CBCT imaging to conduct their study.

It also important to note that there is an easier availability of imaging of TMD subjects, as MRI and CBCT are routinely performed for the diagnosis of those patients (De Leeuw, 2005; Okeson, 2008). CBCT images of orthodontic patients however it is not a routine diagnostic tool (ADA, 2012), as it is still a new imaging modality. This limits the databases available as previously mentioned; as well, when an orthodontic database is available the presence of patients with a particular skeletal malocclusion is not easily attainable. This occurs because the prevalence of skeletal

malocclusions is very small in the general population. The National Health and Nutrition Estimates Survey III (NHANES III) of the United States estimated that severe class II and class III problems at the limit of orthodontic correction (which suggests a skeletal component of the malocclusion) occur in about 4% of the population (Proffit et al, 2007). Granted that the presence of patients with class II and class III skeletal problems are more prevalent in an orthodontic database than in the general population, they likely still represent a smaller percentage.

2.2 Description of cone-beam computed tomography machine

The CBCT machine used was the iCAT® machine (Imaging Sciences International, Hatfield, PA) located within the facilities of the University of Alberta Orthodontic Graduate Program (as described above, CBCT scans are part of the standard record for orthodontic diagnosis and treatment planning at this institution, and appropriate patient consent was acquired).

The CBCT images studied were taken before commencing orthodontic treatment. Patients were instructed to remain still during the image capture procedure with teeth in maximum intercuspation (MI). In case the patient did not maintain dental contact, either due to forward jaw posturing or mouth opening, the process was repeated. Appropriate lead apron shields for gonad and visceral organ protection were used during the procedure.

The parameters used to take the CBCT images included:

- ✓ Slice thickness for primary reconstruction standardized at 0.3mm
- ✓ Collimation height scan of 13 centimeters

- ✓ Scan time of 20 seconds
- ✓ Resolution of at least 0.3 millimeter voxel size
- ✓ The device was operated at the 110 kV (peak)
- ✓ mA settings fixed based on the individual subjects body weight

The field of reconstruction enabled full visualization of the TMJ's, including all aspects of the condyle and glenoid fossa. Scans that had a restricted field of view, limiting considerations regarding the TMJ's were not used. CBCT scans with any motion artifact (caused by patient movement during imaging capture) were excluded. CBCT scans with the patient not in maximum dental intercuspation were excluded as the 90 patients were being selected for the study.

2.3 Description of Imaging Software

Each image acquired by the iCAT machine was obtained from approximately 430 slices and converted to a DICOM format. The DICOM format images were turned into a volumetric image using the cone-beam software platform AVIZO® (VSG®, Berlin, Germany), which allowed for three-dimensional reconstruction of the image, and therefore, the visualization of sagittal, axial, and coronal slices, as well as 3D reconstruction of the image. This software also allows for landmark selection, and provides a predetermined coordinate system and origin (0, 0, 0) for each landmark, which can be transported to a Microsoft Excel® software spreadsheet for the analysis of distances and angles.

Right and left TMJ's in each patient were analyzed in the axial, coronal and sagittal planes, totaling 180 joints. Nine landmarks were selected for each joint, with

a total of 18 landmarks per patient, which will be explained in detail in the subsequent section. Following the landmark selection, the coordinates for each of the landmarks in the axial (x-axis), coronal (y-axis), and sagittal (z-axis) planes were obtained from the AVIZO® software.

Once coordinates were collected, the data was transferred to a Microsoft Excel® software spreadsheet. Linear and angular measurements within and between the condyle and glenoid fossa landmarks were obtained using geometric and trigonometric equations, also with the aid of Microsoft Excel® software. The statistical analysis of the angular and linear measurements obtained was subsequently statistically analyzed.

2.4 Three-dimensional Analysis of the temporomandibular joint

There have been several studies in the literature that proposed different methodologies to achieve a two-dimensional radiographic evaluation of the condyle position in relation to the glenoid fossa (Blashke & Blashke, 1981; Pullinger & Hollender, 1985; Pullinger & Hollender, 1986; Gianelly et al, 1988; Brand et al, 1989; Cohlimia et al, 1996; Katsavrias & Halazonetis, 2005).

The tomographic studies conducted by Pullinger & Hollender (1985, 1986) deserve special attention for the methodology that became the basis for subsequent studies by other authors (Bonilla-Aragon et al, 1999; Pereira & Gaviao, 2004; Menezes et al, 2008). Pullinger & Hollender (1985, 1986) found that the method of linear measurement of the subjective closest posterior and anterior articular space was found to be easy to use and to have a high repeatability. Their results also showed that

this method closely correlated with the subjective scoring with the advantage of demonstrating less inter-observer variation.

The advent of three-dimensional technology, initially with medical grade computed tomography and magnetic resonance imaging, and later with CBCT created an opportunity to evaluate the TMJ in three planes of space. Most studies, however, relied on two-dimensional methodologies to carry out their evaluations (Alexander, Moore & Dubois, 1993; Seren et al, 1994; Bonilla-Aragon et al, 1999; Vitral & Telles, 2002; Vitral et al, 2004; Rodrigues, Fraga & Vitral, 2009; Rodrigues, Fraga & Vitral, 2009; Krisjane et al, 2009; Ikeda & Kawamura, 2009; Vitral et al, 2011; Ikeda & Kawamura, 2011; Sumbulu et al, 2012, Dalili et al; 2012).

A literature review conducted by Stamm et al (2004), on the three-dimensional (3D) physiological position of the temporomandibular joint, concluded that the most frequently found methodology for condyle-fossa position to be the analytic assessment in a two-dimensional (2D) projection of a sagittal plane elected subjectively, even though many of those studies used 3D data.

The present study's landmarks selection was conducted by scrolling through the three planes of space using the AVIZO® software, in order to assure a 3D evaluation as described by Lagravere et al (2009) and Gribel et al (2011). In this system (Cartesian orientation), the XY-plane moves from top to bottom (axial - Figure 1), the XZ-plane moves from front to back (coronal - Figure 2), and the YZ-plane moves from left to right (sagittal - Figure 3). Using this technique allowed the identification of different landmarks in the condyle and glenoid fossa surface that did not necessarily belong to the same computed tomographic slice. This allowed for the

assessment of the three-dimensional relationship between the TMJ condyle and glenoid fossa, as well as the three-dimensional evaluation of these structures separately. Thus, no subjective sagittal, coronal or axial slice selection was conducted for the evaluation of the condyle and glenoid fossa, as has been done in previous studies.

During the landmark selection in the three planes of space the sagittal plane was used for primary orientation to verify the position of the landmarks. This choice was made because this is the plane commonly used for the traditional cephalometric analysis using plain radiographs, which allows the investigator to be more comfortable with the initial selection of landmark points. The coronal and axial planes were subsequently used for the verification of the landmark positioning, and if necessary adjustments were made. Lastly the reconstructed image option ("isosurface") was selected and the landmark selection was verified one last time. Both TMJ's of all subjects were analyzed, starting from the left side first, and always following a pre-determined order of landmarks selection.

Figure 1 Three-dimensional Cartesian system orientation – axial (X-Y)

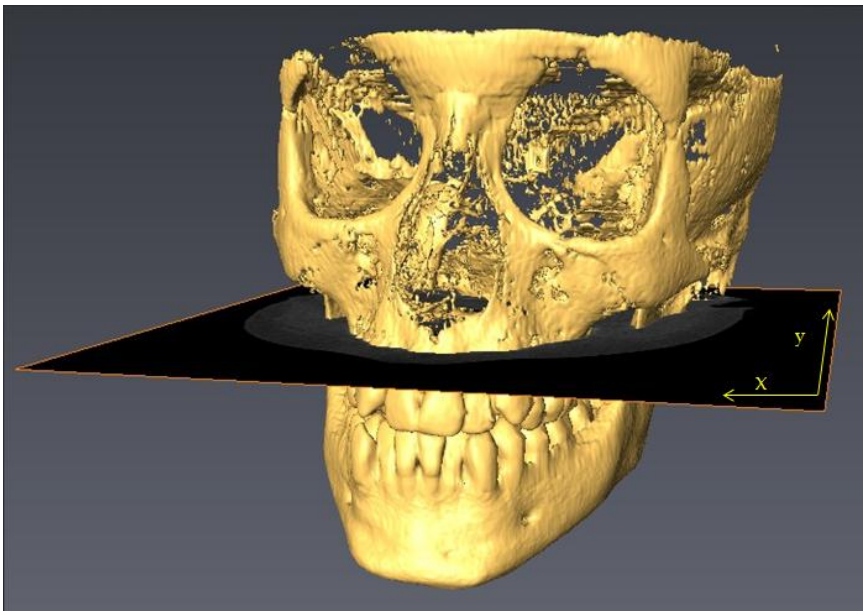

Figure 2 Three-dimensional Cartesian system orientation – coronal plane (X-Z)

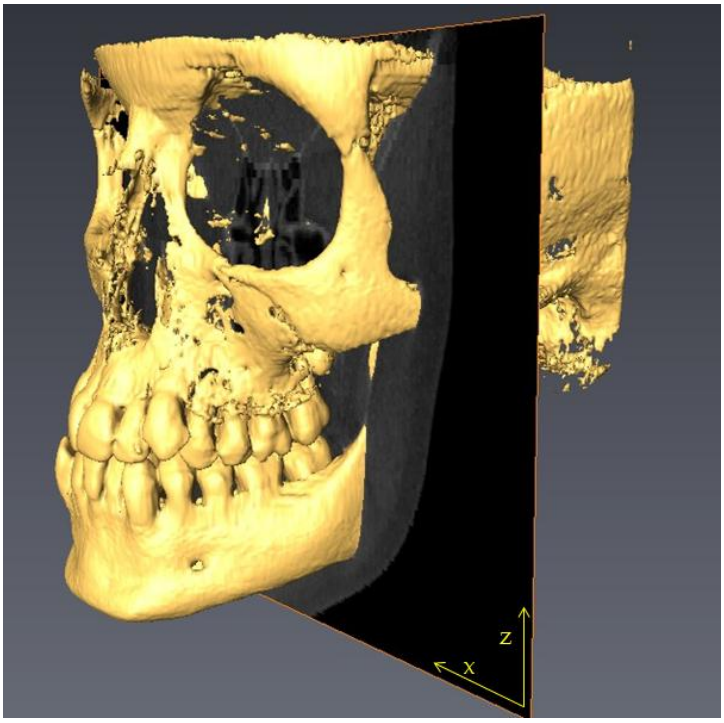

Figure 3 Three-dimensional Cartesian system orientation – sagittal plane (Z-Y)

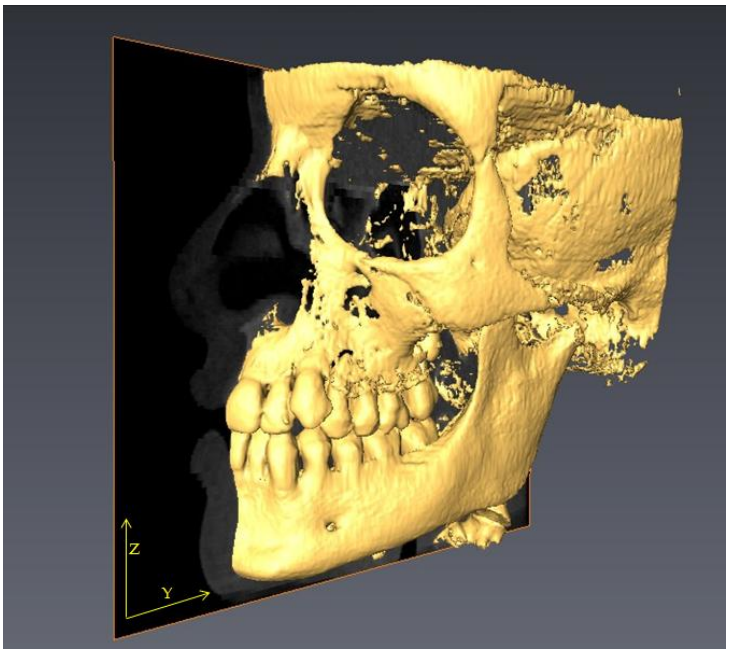

2.4.1 Landmarks definition and selection. The definition of landmarks was based on the information from early studies by Pullinger & Hollender (1995, 1996), and the most up-to-date literature on the evaluation of the TMJ condyle-fossa relationship (Vitral & Telles, 2002; Vitral et al, 2004; Rodrigues, Fraga & Vitral, 2009; Rodrigues, Fraga & Vitral, 2009; Krisjane et al, 2009; Ikeda & Kawamura, 2009; Vitral et al, 2011; Ikeda & Kawamura, 2011; Sumbulu et al, 2012, Dalili et al; 2012).

Table 2 summarizes the definition of the 8 landmarks selected in each plane of space. It also provides CBCT scan pictures to illustrate the position of each landmark in the axial, coronal, and sagittal planes of space, respectively.

Table 2 Landmark definition

Anatomic Region	**Landmark Name**	**Axial view**	**Coronal view**	**Sagittal View**
Lateral pole of the TMJ condyle	L1 (left) R1 (right)	Lateral-most point in the head of the condyle	Lateral-most point in the head of the condyle	Lateral-most point in the head of the condyle
Axial *Coronal* *Saggital* 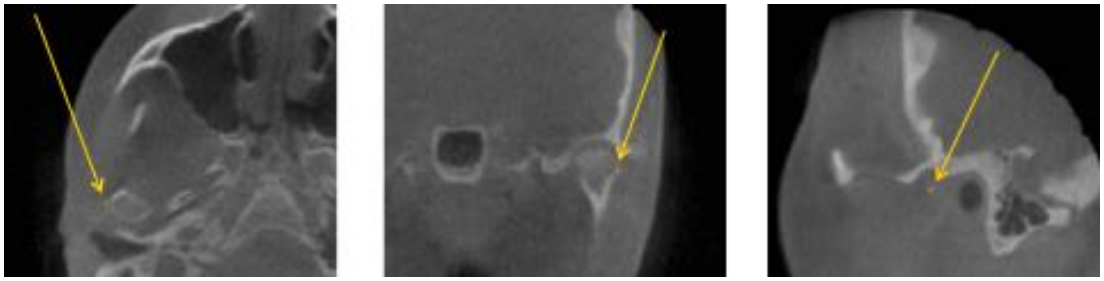				
Anterior pole of the TMJ condyle	L2 (left) R2 (right)	Anterior-most point between the lateral poles of the condyle head	Middle-anterior-most point of the condyle head	Anterior-most point of the condyle head
Axial *Coronal* *Saggital* 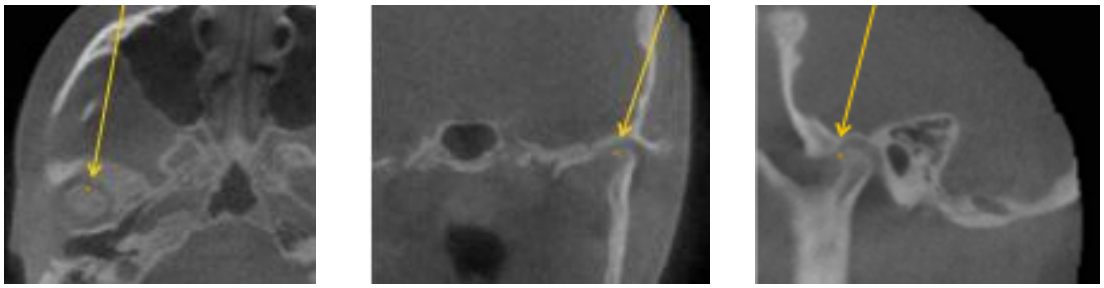				
Superior pole of the TMJ condyle	L3 (left) R3 (right)	Middle point between the lateral poles of the condylar head	Middle-superior-most point of the condyle head	Superior-posterior-most point of the condyle head

Axial  *Coronal* 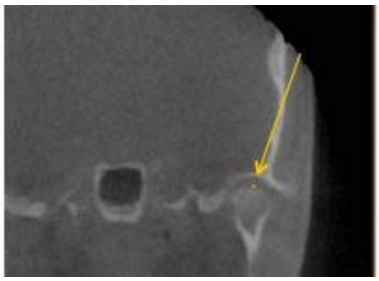 *Saggital* 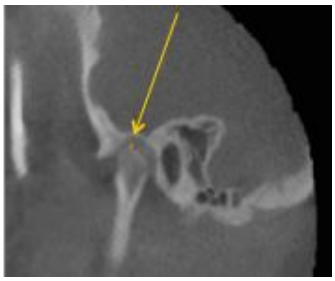				
Posterior pole of the TMJ condyle	L4 (left) R4 (right)	Posterior-most point between the lateral poles of the condyle head	Middle-posterior-most point of the condyle head	Posterior-most point of the condyle head
Axial  *Coronal* 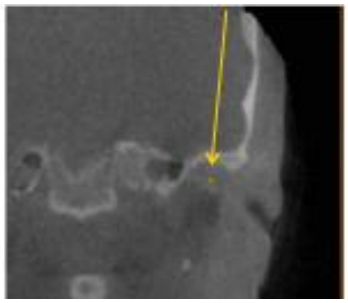 *Saggital* 				
Medial pole of the TMJ condyle	L5 (left) R5 (right)	Medial- most point in the head of the condyle	Medial- most point in the head of the condyle	Medial- most point in the head of the condyle
Axial 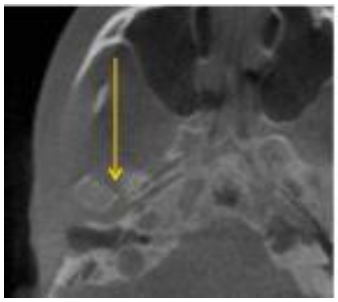 *Coronal*  *Saggital* 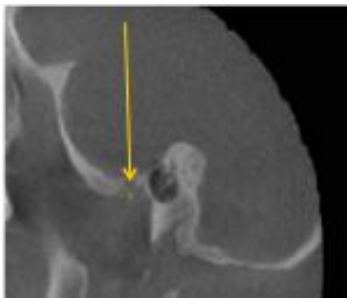				
Inferior pole of the TMJ articular eminence	L6 (left) R6 (right)	Inferior-most point of the articular eminence	Inferior-most point of the articular eminence	Inferior-most point of the articular eminence

Axial		*Coronal*		*Saggital*
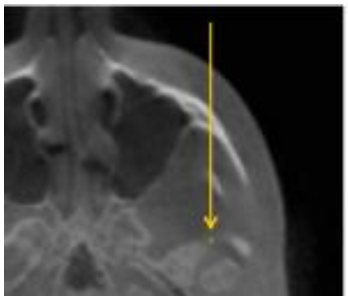				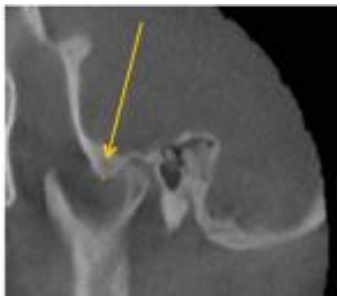
Anterior TMJ fossa	L7 (left) R7 (right)	Anterior-most point on the posterior wall of the articular tubercle	Anterior-most point on the posterior wall of the articular tubercle	Anterior-most point on the posterior wall of the articular tubercle
Axial		*Coronal*		*Saggital*
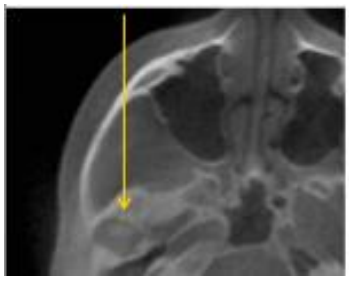		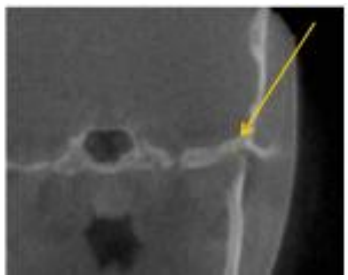		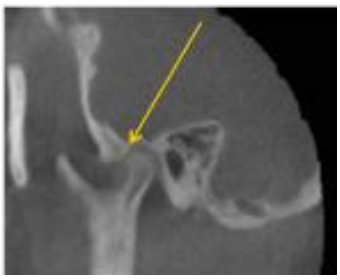
Superior TMJ fossa	L8 (left) R8 (right)	Superior-most point in the posterior wall of the glenoid fossa	Superior-most point in the posterior wall of the glenoid fossa	Superior-most point in the posterior wall of the glenoid fossa
Axial		*Coronal*		*Saggital*
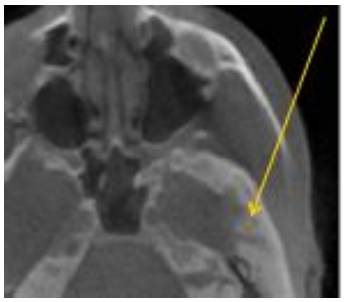		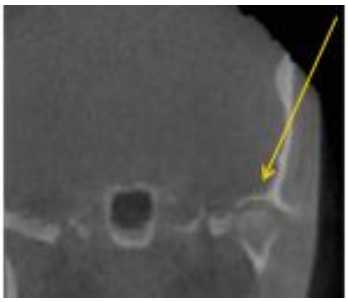		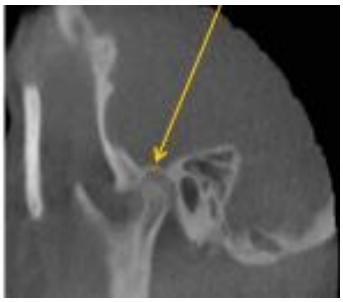

Posterior TMJ fossa	L9 (left) R9 (right)	Posterior-most point in the posterior wall of the glenoid fossa	Posterior-most point in the posterior wall of the glenoid fossa	Posterior-most point in the posterior wall of the glenoid fossa

Axial *Coronal* *Saggital*

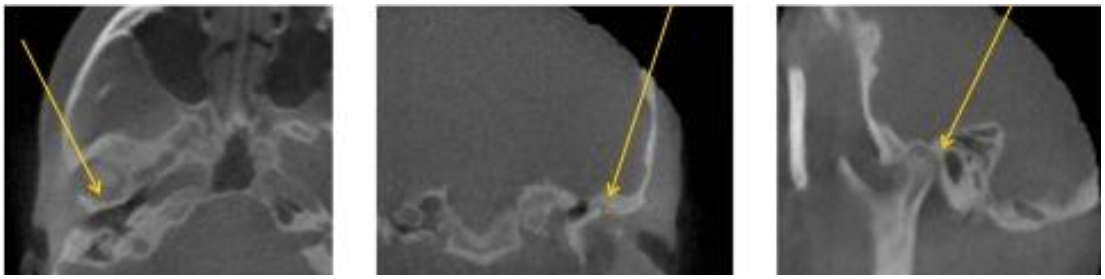

The selection of the 9 landmarks described in table 2 was conducted for each TMJ by the principal investigator, with a total of 180 joints analyzed for 90 patients. No more than 20 joints were analyzed per day to avoid examiner fatigue. Prior to conducting the landmark selection, intra-rater and inter-rater reliability was carried out, which is described in detail in the next section.

After the selection of landmarks for a given patient was completed, the coordinate system and origin (0, 0, 0) was acquired for each image with the AVIZO® software. Each landmark received an alphanumerical name as seen in table 2 and transported to a Microsoft Excel® software. This helped to successfully undertake the calculations of linear and angular measurements.

2.4.2 Inter and intra-rater reliability. The assessment of inter-rater and intra-rater reliability was conducted using a sample of 10 subjects from the poll of the 90 CBCT scans selected for this study. The scans were selected randomly from the 3 groups studied.

Intra-reliability is defined as the extent of which test results from a given subject are stable over time when administered by the same investigator (Ljunquist, Harms-Ringdahll & Nygun, 1999). The principal investigator conducted the landmarks selection for a given subject on three different occasions. Each occasion separated by at least 1 week, and blinded from the previous evaluation.

Inter-reliability is defined as whether different investigators are capable of obtaining comparable measurements when assessing a given subject (Ljunquist, Harms-Ringdahll & Nygun, 1999). This was determined by having an expert in the field (M.L.) of three-dimensional analysis conduct the landmark selection for the same 10 scans analyzed by the principal investigator. In addition, an undergraduate dental student (J.S.) with experience in three-dimensional analysis was trained to conduct the landmark selection for the same 10 scans. These investigators were blinded from the principal investigator's landmark selection and located the landmarks on a single occasion.

Following the inter-rater and intra-rater reliability studies, the data was inputted into an Excel® file for statistical analysis, which is described in more detail in the next chapter of this text. The second scoring of the intra-reliability was chosen to perform the statistical analysis for inter-rater reliability, as it is not the first scoring that may contain errors, nor the last scored that is being repeated for the third time and may contain more bias. The data analysis was performed using the SPSS statistical package system version 17.0 (Chicago, IL, USA).

2.4.3 Linear and angular measurements. The linear and angular measurements proposed by the present study aimed to be a simple method that could

be easily repeated in future research and in the clinical setting by both clinicians and support staff.

The anterior (D1), superior (D2) and posterior (D3) joint spaces were calculated by measuring the distance between the anterior, superior and posterior poles of the condyle to the anterior, superior and posterior landmarks in the glenoid fossa respectively (figure 4). For example, for the left anterior joint space (AJS-L), the distance between the anterior pole of the left TMJ condyle (L2) to the anterior-most point of the TMJ fossa (L7) there are distances in the x, y and z coordinates (e.g. L2x to L7x, L2y to L7y, AND L2z to L7z). An excel function was used to convert the linear distances achieved between each coordinate and transform it into one single linear distance for each joint space as shown in the following equation:

*D1 (linear distance from L2 to L7) = Square Root ((L2x-L7x) * (L2x-L7x) + (L2y-L7y) * (L2y-L7y) + (L2z-L7z) * (L2z-L7z))*

The same equation concept was used for the calculations of superior joint spaces (D2) and posterior joint spaces (D3).

Figure 4 Anterior (D1), superior (D2) and posterior (D3) joint spaces

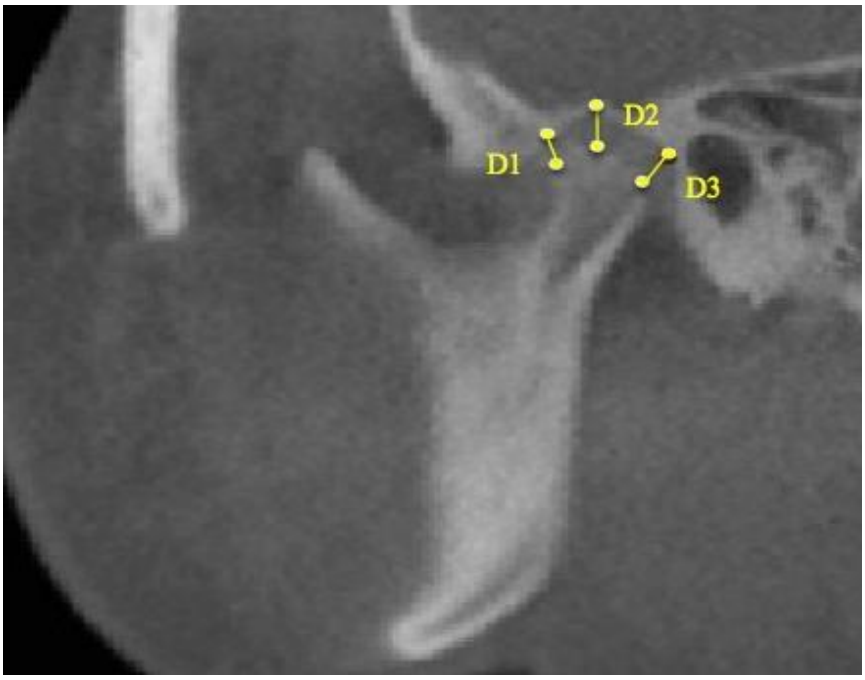

The angle of the condyle was assessed though the measurement of the distances from the anterior condyle pole to the superior condyle pole (D4), the distance from the superior pole to the posterior pole (D5), and the distance from the posterior pole to the anterior pole (D6) as seen in figure 5. A triangle was then formed, and subsequently the angle at the superior condyle pole landmark (A1) was calculated using the following equation:

Anti-cosine = [(D4 x D4) + (D5 x D5) – (D6 x D6)] / 2 x D4 x D5

The results achieved were described in radians and later converted to degrees using a Microsoft Excel® software function; the larger the angle the flatter the superior condylar angle.

Figure 5 Condyle angle

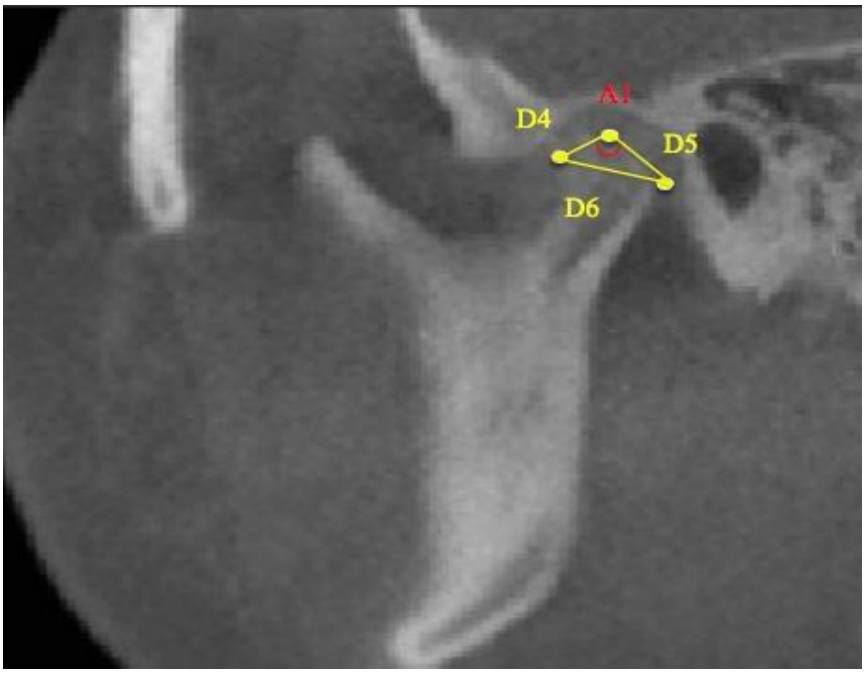

The angle of the fossa was assessed though the measurement of the distances from the anterior fossa landmark to the superior fossa landmark (D7), the distance from the superior fossa landmark to the posterior fossa landmark (D8), and the distance from the posterior fossa landmark to the anterior fossa landmark (D9) as seen in figure 6. A triangle was then formed, and subsequently the angle at the superior fossa landmark (A2) was calculated using the following equation:

$$Anti\text{-}cosine = [(D7 \times D7) + (D8 \times D8) - (D9 \times D9)] / 2 \times D7 \times D8$$

The results achieved were described in radians and later converted to degrees using a Microsoft Excel® software function; the larger the angle the flatter the fossa angle.

Figure 6 Fossa angle

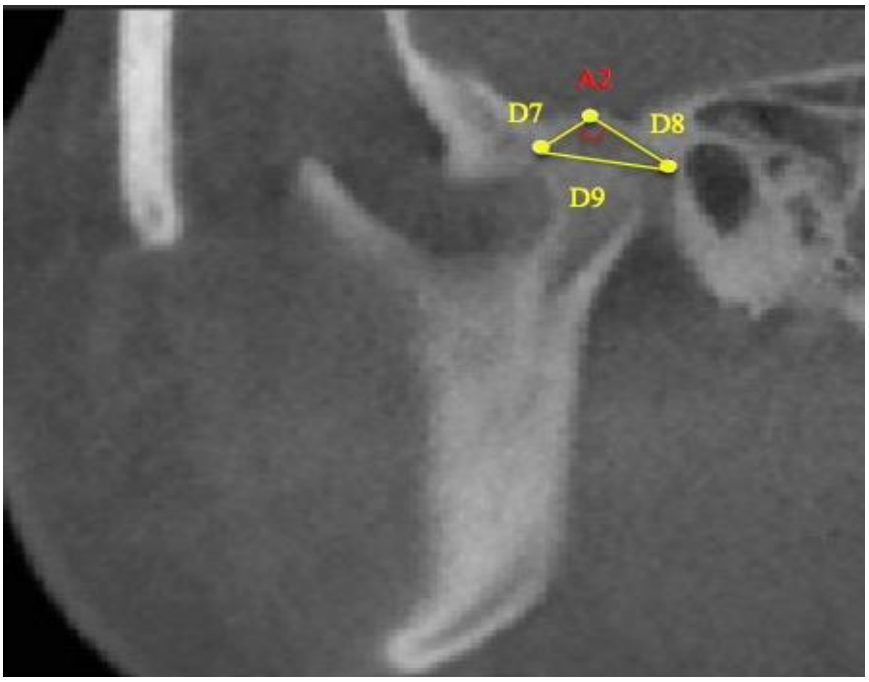

The depth of the glenoid fossa (D13) was done through the measurement of the distances from the articular eminence landmark to the superior fossa landmark (D10), the distance from the superior fossa landmark to the posterior fossa landmark (D11), and the distance from the posterior fossa landmark to the articular eminence landmark (D12) as seen in figure 7. A triangle was then formed, and subsequently the anti-cosine (described in radians) of the angle at the posterior fossa landmark (A3) was calculated using the following equation:

$$Anti\text{-}cosine = [(D7 \times D7) + (D8 \times D8) - (D9 \times D9)] / 2 \times D7 \times D8$$

Determining the anti-cosine of angle A3 was necessary to calculate the perpendicular distance from the superior glenoid fossa landmark to the base of the

triangle (D13) using the right triangle rule. The following equation was used to determine D13:

D13 = [Sine (Anti-cosine A3)] x D11

Figure 7 Fossa depth

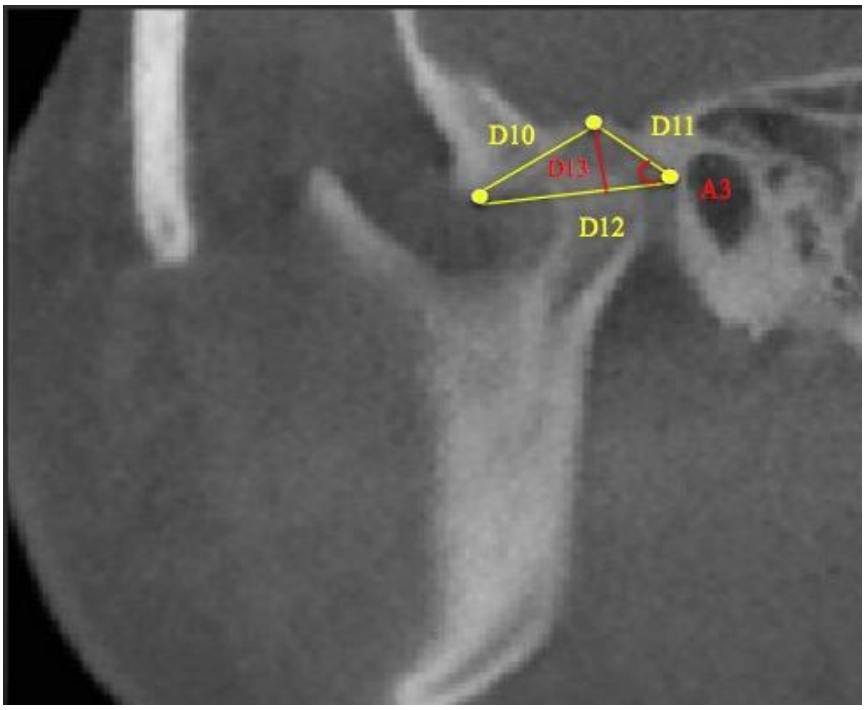

Following the determination of the linear and angular measurements with the aid of the Microsoft Excel® software, the data was organized in a spreadsheet and statistically analyzed using SPSS® software.

2.5 Statistical Analysis

Intra-examiner reliability values were determined by using two-way mixed absolute agreement Intra-class Correlation Coefficients (ICCs), to assist in the

identification of reliability of the main investigator during three different time points Cronbach's Alpha Statistics was also calculated.

The ICC was the reliability test chosen firstly because the present study aims to compare different sets of quantitative data. Secondly, due to the argument that ICC performs very well in the appraisal of agreement in terms of consistency and conformity of two quantitative measurements in a situation that none of them is seen as the gold standard (Muller & Buttner, 1994), which is the situation seen in the present study.

In addition to ICC, Cronbach's alpha Statistics was chosen to aid in the assessment of reliability in the present study. This test is valuable in the assessment of reliability in the particular situation where item-specific variance in a one-dimensional test is the matter studied (Cortina, 1993), which are the circumstances seen in the present study.

In terms of the evaluation of the reliability, Sharout (1998) proposes a revision to the evaluation of reliability described by Landis and Koch (1997), as follows: 0.00 to 0.10 - virtually none; 0.11 to 0.40 - slight; 0.41 to 0.60 - fair; 0.61 to 0.80 - moderate; 0.81 to 1.00 – substantial. This is the reliability evaluation definition used in the present study.

Inter-examiner reliability values were determined by using Intra-class Correlation Coefficients (ICCs), to assist in the identification of reliability of the landmarks proposed by this study among different raters Cronbach's Alpha Statistics was also calculated. For the purposes of the statistical calculations the raters are

described in the following tables as such: “2” (main investigator’s second evaluation time point), “m” (expert investigator), “j” (undergraduate student investigator).

The values found for each of the measurements was organized in a Microsoft Excel spreadsheet and separated into three groups (class I, class II and class III). Descriptive statistics was applied to the data set using SPSS statistical package. Kolmogorov-Smirnov test showed that the data had a normal distribution; thereafter the measurements were compared within the groups and between groups using repeated measures ANOVA and all the pairwise comparisons using the Bonferroni method.

In order to assess whether there was a statistical significant difference between the measurements studied repeated ANOVA testing was applied (table 26) using a $p < 0.05$. The Bonferroni pairwise comparison test was carried-out with the objective of determining where exactly the statistical differences for AJS-L and FD-L was located in terms of the groups studied.

Chapter III

Results

3.1 Reliability of TMJ Landmark Selection

3.1.1 Intra-reliability. Intra-examiner reliability for x, y and z coordinates for all landmarks ranged from 0.99 to 1.00 with 95% confidence interval according to ICC. The intra-examiner reliability for x, y and z coordinates for all landmarks ranged from 0.99 to 1.00 according to Cronbach's alpha Statistics values. The reliability assessed by intra-reliability tests attested substantial agreement of the 3 evaluations carried-out by the main investigator, assuring the repeatability by the same investigator of the landmarks proposed by the present study.

Intra-examiner reliability for x coordinated varied from 0.99 to 1.00 with a 95% confidence interval for all landmarks studied (Appendix 2 - table 3 and table 4). Cronbach's alpha Statistics for x coordinate varied from 0.99 to 1.00 (Appendix 2 - table 5).

Intra-examiner reliability for y coordinated varied from 0.99 to 1.00 with a 95% confidence interval for all landmarks studied (Appendix 2 - table 6 and table 7). Cronbach's alpha Statistics for y coordinate varied from 0.99 to 1.00 (Appendix 2 - table 8).

Intra-examiner reliability for z coordinated varied from 0.99 to 1.00 with a 95% confidence interval for all landmarks studied (Appendix 2 - table 9 and table 10). Cronbach's alpha Statistics for x coordinate was 1.00 for all landmarks (Appendix 2 - table 11).

3.1.2 Inter-reliability. Inter-examiner reliability for x, y and z coordinates for all landmarks ranged from 0.55 to 1.00 with 95% confidence interval according to ICC. The ICC for x, y and z coordinates for all landmarks ranged from 0.78 to 1.00

according to Cronbach's alpha Statistics values. The reliability assessed by the ICC test attested moderate to substantial agreement between the raters for all but one landmark in one specific coordinate (e.g. landmark 9 – left posterior TMJ fossa, z coordinate). The reliability assessed by Cronbach's alpha Statistics, however, attested moderate to substantial agreement between raters for all landmarks and coordinates. The results of the inter-reliability tests assessed moderate to substantial repeatability by different investigators of the landmarks proposed by the present study.

Inter-examiner reliability for x coordinated varied from 0.99 to 1.00 with a 95% confidence interval for all landmarks studied (Appendix 2 - table 12 and table 13). Cronbach's alpha Statistics for x coordinate was 1.00 for all landmarks (Appendix 2 - table 14).

Inter-examiner reliability for y coordinated varied from 0.99 to 1.00 with a 95% confidence interval for all landmarks studied (Appendix 2 - table 15 and table 16). Cronbach's alpha Statistics for y coordinate varied from 0.99 to 1.00 (Appendix 2 - table 17).

Inter-examiner reliability for z coordinated varied from 0.55 to 1.00 with a 95% confidence interval for all landmarks studied according to ICC. The lower agreement of 0.550 was found for landmark 9 (left posterior TMJ fossa) only. The remaining landmarks show an agreement varying from 0.78 to 1.00, where most of the landmarks show an agreement of 0.99 or higher (Appendix 2 - table 18 and table 19). Cronbach's alpha Statistics for z coordinate varied from 0.78 to 1.00 for all landmarks (Appendix 2 - table 20). The differences found in the raw data are smaller than 1mm, and therefore unlikely to be of clinical significance.

3.2 Three-Dimensional Evaluation of the TMJ Condyle Position Within the Glenoid Fossa in Different Types of Skeletal Patterns

A total of 90 CBCT scans were evaluated from 40 males and 50 females, with a mean age of 19.48 years (10.11 to 36.10 years). The sample of orthodontic patients selected for this study is described on table 21 for gender and age distributions within each group. Table 22 describes the distribution of the cephalometric measurements values used for sample selection within each group.

Table 21 Age and Gender distribution

	Age (average)	**Age (range)**	**Gender**		**Total**
			Male	**Female**	
Class I	23.5 years	11.0 – 36.1 years	12	18	30
Class II	16.0 years	10.1 – 21.2 years	15	15	30
Class III	18.8 years	11.9 – 26.0 years	13	17	30
Total	**19.4 years**	**10.1 – 36.1 years**	**40**	**50**	**90**

Table 22 Distribution of cephalometric measurements values

	OJ (Bjork III)	**ANB**	**Wits**	**Harvold diff.**	**Y-axis**	**MP-SN**	**MP-FH**
Class I							
Average	3.05	2.62	-0.85	27.14	62.69	36.50	24.90
Maximum	6.50	6.50	4.30	35.20	77.70	47.10	35.30
Minimum	-0.60	0.00	-4.90	20.50	52.90	24.40	13.40
Class II							
Average	7.48	5.48	4.68	24.27	68.39	34.69	25.06
Maximum	9.90	9.20	9.90	34.80	78.00	48.20	39.60
Minimum	4.00	2.40	1.30	13.70	57.60	20.90	12.00
Class III							
Average	0.25	-1.14	-6.58	35.23	59.41	34.79	25.33
Maximum	6.80	1.70	-0.40	47.40	78.30	52.10	39.30
Minimum	-9.00	-4.80	-20.40	26.60	51.70	21.70	12.20

The data acquired from the landmark selection provided a value in millimeters for each landmark for the x, y and z coordinates. As explained in Chapter 2, these coordinates were converted into distances and to measure anatomical differences in the condyle, glenoid fossa, and the relationship between these two structures within the same group (right and left sides), and between different groups. Table 23 describes the nomenclature used for the statistical analysis.

Table 23 Measurement nomenclature

	Measurement	Definition	Type
1	**AJS-L**	Anterior joint space – left	Distance (mm)
2	**AJS-R**	Anterior joint space – right	Distance (mm)
3	**SJS-L**	Superior joint space – left	Distance (mm)
4	**SJS-R**	Superior joint space – right	Distance (mm)
5	**PJS-L**	Posterior joint space – left	Distance (mm)
6	**PJS-R**	Posterior joint space – right	Distance (mm)
7	**CA-L**	Condyle angle – left	Angle (degrees)
8	**CA-R**	Condyle angle – right	Angle (degrees)
9	**FA-L**	Fossa angle – left	Angle (degrees)
10	**FA-R**	Fossa angle – right	Angle (degrees)
11	**FD-L**	Fossa depth – left	Distance (mm)
12	**FD-R**	Fossa depth - right	Distance (mm)

The mean values for each of the 12 measurements studied for the class I, class II and class III groups, and their standard deviations are listed on table 25 (Appendix 2). The mean absolute differences between AJS and PJS are as follows: class I left (0.97mm), class I right (1.25mm); class II left (0.5mm), class II right (1.27mm); class III left (0.87mm), class III right (0.7mm). Concentricity is presently defined as anterior and posterior joint spaces being equal or nearly equal (+/- 0.2mm). The results show that the anterior joint spaces were smaller than the posterior joint spaces for all groups, which shows the presence of a non-concentric positioning of the condyle within the glenoid fossa, favoring an anterior positioning of the TMJ condyle

within the glenoid fossa. These differences were proven to be not statistically significant as described below.

Table 24 Descriptive statistics – data distribution

Measure	Mean	Std. Error	95% Confidence Interval	
			Lower Bound	Upper Bound
AJS-L	3.85	.71	2.44	5.25
AJS-R	3.45	.71	2.05	4.85
SJS-L	3.87	.71	2.46	5.27
SJS-R	3.78	.71	2.38	5.18
PJS-L	4.62	.71	3.22	6.03
PJS-R	4.52	.71	3.12	5.93
CA-L	101.98	.71	100.58	103.38
CA-R	103.10	.71	101.70	104.50
FA-L	112.65	.71	111.25	114.05
FA-R	113.62	.71	112.22	115.02
FD-L	4.76	.71	3.36	6.17
FD-R	5.01	.71	3.60	6.41

From the 12 measurements studied, only measurements AJS-L (anterior joint space left) and FD-L (fossa depth left) showed statistically significant differences of 0.018 and 0.006 respectively.

Table 26 Test of between subjects effect – analysis of variance (ANOVA)

Measure		Type III Sum of Squares	df	Mean Square	F	Sig.
AJS-L	Corrected Model	10.23	2	5.11	4.22	**.018**
AJS-R	Corrected Model	2.27	2	1.13	1.26	.287
SJS-L	Corrected Model	7.33	2	3.66	2.46	.091
SJS-R	Corrected Model	5.03	2	2.51	1.47	.235
PJS-L	Corrected Model	1.76	2	.88	.46	.627
PJS-R	Corrected Model	4.00	2	2.00	.86	.424
CA-L	Corrected Model	259.48	2	129.74	1.10	.336
CA-R	Corrected Model	34.06	2	17.03	.20	.813
FA-L	Corrected Model	355.07	2	177.53	.99	.373
FA-R	Corrected Model	161.40	2	80.70	.49	.611
FD-L	Corrected Model	9.13	2	4.56	5.43	**.006**
FD-R	Corrected Model	2.89	2	1.44	1.91	.154

Table 27 (Appendix 2) shows the results of the Bonferroni test, and clarifies that the significant difference found for measurement AJS-L lays between the class I and class II groups. The significant difference found for measurement FD-L, on the other hand, was encountered between class I and class III groups. The p-values assessed by the Bonferroni test for all the remaining measurements when compared between the groups corroborates with the ANOVA findings, with no statistically significant differences seen.

Although there were a statistically significant difference detected for the measurements described in the previous paragraph, when the raw values are studied (appendix 2 – table 25) the mean difference found for AJS-L between class I and class II groups is of 0.81mm, and for FD-L is of 0.75mm (appendix 2 – table 27). These are values smaller than 1mm and therefore unlikely to be of clinical significance.

Additionally, the Bonferroni test was carried-out to compare the groups between each other (table 28), as well as to compare the subjects between each other without separating them into groups (table 29). In both instances there were no statistically significant differences.

Table 28 Multiple comparisons between groups - Post-hoc test - Bonferroni

(I) Class		Mean Diff.	Std. Error	Sig.	95% Confidence Interval	
					Lower Bound	Upper Bound
1.00	2.00	-.39	.50	1.00	-1.60	.82
	3.00	-.09	.50	1.00	-1.30	1.11
2.00	1.00	.39	.50	1.00	-.82	1.60
	3.00	.29	.50	1.00	-.91	1.50
3.00	1.00	.09	.50	1.00	-1.11	1.30
	2.00	-.29	.50	1.00	-1.50	.91

Table 29 Multiple comparisons between variables - Post-hoc test - Bonferroni

(I) Measure		Mean Diff.	Std. Error	Sig.	95% Confidence Interval for Difference	
					Lower Bound	Upper Bound
AJS-L	AJS-R	.39	1.01	1.00	-3.01	3.81
	SJS-L	-.02	1.01	1.00	-3.43	3.39
	SJS-R	.06	1.01	1.00	-3.34	3.48
	PJS-L	-.77	1.01	1.00	-4.19	2.63
	PJS-R	-.67	1.01	1.00	-4.09	2.73
AJS-R	AJS-L	-.39	1.01	1.00	-3.81	3.01
	SJS-L	-.41	1.01	1.00	-3.83	2.99
	SJS-R	-.32	1.01	1.00	-3.74	3.08
	PJS-L	-1.17	1.01	1.00	-4.58	2.24
	PJS-R	-1.07	1.01	1.00	-4.48	2.34
SJS-L	AJS-L	.02	1.01	1.00	-3.39	3.43
	AJS-R	.41	1.01	1.00	-2.99	3.83
	SJS-R	.08	1.01	1.00	-3.32	3.50
	PJS-L	-.75	1.01	1.00	-4.17	2.65
	PJS-R	-.65	1.01	1.00	-4.07	2.75
SJS-R	AJS-L	-.06	1.01	1.00	-3.48	3.34
	AJS-R	.32	1.01	1.00	-3.08	3.74
	SJS-L	-.08	1.01	1.00	-3.50	3.32
	PJS-L	-.84	1.01	1.00	-4.26	2.56
	PJS-R	-.74	1.01	1.00	-4.16	2.66
PJS-L	AJS-L	.77	1.01	1.00	-2.63	4.19
	AJS-R	1.17	1.01	1.00	-2.24	4.58
	SJS-L	.75	1.01	1.00	-2.65	4.17
	SJS-R	.84	1.01	1.00	-2.56	4.26
	PJS-R	.10	1.01	1.00	-3.31	3.51
PJS-R	AJS-L	.67	1.01	1.00	-2.73	4.09
	AJS-R	1.07	1.01	1.00	-2.34	4.48
	SJS-L	.65	1.01	1.00	-2.75	4.07
	SJS-R	.74	1.01	1.00	-2.66	4.16
	PJS-L	-.10	1.01	1.00	-3.51	3.31
CA-L	CA-R	-1.12	1.01	1.00	-4.53	2.29
CA-R	CA-L	1.12	1.01	1.00	-2.29	4.53
FA-L	FA-R	-.97	1.01	1.00	-4.38	2.44
FA-R	FA-L	.97	1.01	1.00	-2.44	4.38
FD-L	FD-R	-.24	1.01	1.00	-3.65	3.17
FD-R	FD-L	.24	1.01	1.00	-3.17	3.65

Chapter IV

Discussion

4.1 Three-Dimensional Evaluation of the TMJ Condyle Position Within the Glenoid Fossa in Different Types of Skeletal Patterns

The methodology used in the present study aimed to correct the drawback of previous researches on TMJ condyle-fossa relationship pointed out by Stamm et al (2004). A 3D study of the TMJ was designed using the three-dimensional landmark evaluation technique described by Lagravere et al (2009) and Gribel et al (2011) using a Cartesian orientation system through the imaging software AVIZO, which allowed the selection of landmarks that did not necessarily belong to the same CT slice. This software also provided the coordinates for the x, y and z planes for each landmark.

The study of the anatomical structures of the TMJ in all 3 planes of space allowed for the calculation of the distances in two dimensions, as well as determining angulations of anatomical structures. This permitted for the drawing of a clearer picture of the condyle-fossa relationships. Those areas of the methodology allowed for a 3D evaluation of the TMJ that has not yet been published in the literature. Endo et al (2011) study presented a 3D evaluation of the TMJ that used reconstructed images. They however used CT imaging, which is a more expensive technology (Honda, 2006), as well as it exposes the patient to increased radiation (Ludlow, Davies- Ludlow & Brooks, 2003; Schulze et al, 2004; Tsiklakis, Syriopoulos & Stamatakis, 2004). Other important drawback of their methodology lies on the fact that 1mm slice thickness was used, which introduces considerable error in both the coronal and sagittal plane (Angelopoulos, Scarfe & Farman, 2012).

It is critical, however, to stress the fact that the three planes of space (x, y and z axis) were evaluated concomitantly in the present study as a method of assessment of the three dimensions of the anatomical structures, with the subsequent calculation of the 2D distances between the anatomical structures, as well as angulations of the surface anatomy of TMJ condyle and fossa. Although a 3D evaluation was carried-out in a way, this cannot be defined as a "true" 3D evaluation, as the actual visualization and measurement of the TMJ anatomical structures as a whole was not done, such as the evaluation of a given anatomical structure *in vivo* or in a cadaver model for example.

The assessment of intra-reliability and inter-reliability for the landmark placement for the TMJ condyle and glenoid fossa proposed demonstrated adequate reproducibility for all landmarks placement made by the same investigator, as well as adequate repeatability of all the landmarks placement conducted by three different investigators. Based on these results it was possible to infer that the 3D TMJ landmark evaluation presented can adequately be carried-out by other investigators either clinically or in future research.

The results found that as for the absolute mean values for the anterior and posterior joint spaces found for the entire sample there was a non-concentric positioning of the condyle, favoring a smaller anterior joint space. The different skeletal patterns showed similar differences between absolute anterior and posterior joint spaces. This allowed the interpretation that there were very small dissimilarities (< 1.27mm) in the differences between the mean AJS and PJS values for the skeletal

class I, class II and class III sample studied, which are unlikely to be of clinical significance.

Concentricity was presently defined as anterior and posterior joint spaces being equal or nearly equal (+/- 0.2mm), this is a very small difference, but for the purposes of assessing concentricity it appears to be useful. The matter of clinical significance of the differences found in the joint spaces, on the other hand, is a very difficult point to determine with certainty, as it is a very difficult issue to study either clinically or radiographically, and has not yet (to our knowledge) been published in the literature. This is true because of the individual variability of the TMJ joint spaces, where a difference of 1mm or less in the AJS and PJS may not be clinically significant to affect the condyle position to the point of putting the articular disk in risk of displacement, for example, but it can be severe enough for others. As found by Saccuci et al (2012), the volume of the condylar head was found to differ in different skeletal patterns (class II < class III) and in different genders (females < males). Would the glenoid fossa differ in the same proportion as the condyle for those individuals, or smaller/larger articular spaces could be seen for those patients? This is a question that perhaps would be best answered in terms of percentages, rather than absolute numbers.

The findings of non-concentricity in the current study corroborate with results achieved by Alexander, Moore and Dubois (1993) that found non-concentricity of the TMJ condyle in 50% of their sample of dental class I patients using magnetic resonance imaging (MRI). Cohlimia et al (1996) used tomograms for their analysis and found the position of the TMJ condyle to be non-concentric within the glenoid

fossa for their skeletal and dental class I, class II and class III groups. Katsavrias & Halazonetis (2005) also used tomograms to analyze the condyle-fossa relationship of a skeletal class II skeletal and class III groups; their results showed a non-concentric position of the condyle for all groups. All those studies however used a 2D methodology to conduct their condyle-fossa measurements.

Other authors used medical grade CT technology and found similar results, such as Seren (1994), that found non-concentricity of the condyle-fossa relationship in his skeletal class III sample. Rodrigues, Fraga & Vitral (2009) found the condyle-fossa relationship to be non-concentric for both class II and class III dental malocclusion groups. Rodrigues, Fraga & Vitral (2009) found non-concentricity of their dental class I malocclusion sample. Vitral et al (2011) evaluated a sample of TMD-free, class I normal occlusion subjects and found the condyle-fossa relationship of those patients to be non-concentric. Krisjane et al (2009) found non-concentricity for both the skeletal class II and class III groups evaluated. Once again, all those studies used a 2D methodology to conduct their condyle-fossa measurements.

Dalili et al (2012) disagrees with the results of condyle-fossa non-concentricity assessed by the present study and the other studies mentioned previously for a class I skeletal sample. They conducted a study using CBCT technology and evaluated the TMJ condyle-fossa relationship through the analysis of a 2D sagittal and coronal slice. These authors analyzed a sample of skeletal class I subjects and reported a centric position of the condyle to be the most common in their sample. This perhaps occurred because they used a 2D evaluation of the 3D CBCT images they had from their patient pool. Even though they assessed both the sagittal

and coronal view, this was done independently and does not apply as 3D evaluation as was performed by the present study.

Although the mean values for the anterior and posterior joint spaces found for the groups studied evidenced a smaller anterior joint space when compared to the posterior joint space, when statistical analysis were carried-out to assess the significance of the differences found between the means of each measurement there was no statistically significant differences found ($p < 0.05$) between the groups or between the sides within each group. With the exception of 2 measurements: anterior joint space – left (AJS-L), and fossa depth – left (FD-L).

When post-hoc Bonferroni test was carried out it was detected that the statistically significant difference found by ANOVA for AJS-L occurred between class I and class II groups. For the FD-L measurement the Bonferroni test detected that the statistically significant difference found by ANOVA for FD-L occurred between the class I and class III groups. The class I group had a FD-L on average 0.7517mm larger than the class III group. When the raw data was studied, the differences found for both measurements were smaller than 1mm and therefore unlikely to be of clinical significance. It should also be taken into consideration the measurement error, inherent to the software use and operator's landmark selection. This is important to consider as with those factors added to the equation these differences are likely even smaller in reality.

It is interesting to note that both measurements found to have a statistically significant difference was located on the left side. Cohlimia et al (1996) credited asymmetries found between right and left TMJ's to possibly be a factor of normal

cranial base asymmetries and the likelihood that most patients favor one particular side during mastication. In the present situation, however, the difference was not seen between the left and right sides for the same measurement, but for the left side between different skeletal patterns. It is unfortunately not possible to draw an inference for the reason why only the left side was found as being significantly different for AJS between class I and II, and for FD between class I and III; this appears to be a random finding as there is no report in the literature of only one TMJ side being particularly favored by differences between skeletal patterns.

It also important to note that although in the evaluation of the mean values for the measurements studied there were smaller anterior joint spaces in comparison to posterior joint spaces, the study of the results of the Bonferroni post-hoc test showed that these differences were not statistically significant. This does not mean, however, that the condyle was in a centric position, but that the differences found were not statistically significant to necessarily draw a conclusion that the condyle was significantly positioned more anteriorly, posteriorly or superiorly in a particular group. It is also worth adding that the differences found in the mean values were so small (between 0.5mm to 1.27mm) that they are unlikely to be of clinical significance. And again they could be smaller considering operator error. This however is a subjective statement, as described previously, as the extent of difference needed in the anterior and posterior joint space to classify it as clinically significant has not yet been determined in the literature.

These results contradict previous findings by Seren (1994) and Cohlimia et al (1996) that found their skeletal class III samples to present a more anterior condylar

position; Katsavrias & Halazonetis (2005) that found their class II skeletal (class II division one dental) group to present a more anterior condylar position, and his class II skeletal (class II division 2 dental) to present a more posterior condylar position; and Krisjane et al (2009) that found a more anteriorly positioned condyle for both skeletal class II and class III groups studied. These different findings can be credit to differences in methodologies between the above studies and the current study, such as differences in sample size, imaging technique, and particularly the lack of a true 3D evaluation of the anatomical structures. Seren (1994) and Krisjane et al (2009) evaluated a small sample (39 and 29 subjects respectively), and used a 2D evaluation of CT images. Cohlimia (1996) and Katsavrias & Halazonetis (2005) evaluated a large sample (232 and 189 subjects respectively), but analyzed only 2D slices from linear tomograms.

Conversely, other studies corroborate with findings of non-concentricity with no statistical significant support that one direction in particular was being favored, such as Cohlimia (1996), for his skeletal class I and class II groups; Vitral et al (2004), for their dental class II division 1 subdivision sample; Rodrigues, Fraga & Vitral (2009), for their dental class II division 1 and class III groups; Rodrigues, Fraga & Vitral (2009) for their dental class I malocclusion sample; and Vitral et al (2011) for their dental class I normal occlusion sample. The last four studies had 30 subjects for each of their groups, and used a 2D evaluation of CT images. It is however difficult to make a direct comparison from those studies to the present study as they used different sample sizes, imaging techniques, and more importantly, did not assessed the anatomical structures in a 3D manner.

The results of comparisons between condyle angle and fossa angle between different sides and different skeletal patterns showed that there were no statistical significant differences in those variables. Katsavrias & Halazonetis (2005), on the other hand, found the condyle shape for their skeletal class III group to be more elongated than the class II group; they also found the fossa shape for the class III group as shallower than the class II group. These divergent findings can be attributed to differences in methodology as explained previously.

4.2 Limitations of the study and recommendations for future research

The biggest limitation in the present study lies on the operator landmark selection error, as well as error related to distortions created by CBCT imaging possibly brought by inherent issues of this technology, such as partial voxeling. Although the literature has found that linear measurements taken with the use of CBCT technology are reliable (Periago et al, 2008; Brown et al, 2009), and the present study found adequate intra and inter reliability, the TMJ joint spaces are so minute that even a small error has the potential of creating a large discrepancy when clinical differences are taken into account. Some studies on the linear accuracy of CBCT (Periago et al, 2008; Brown et al, 2009) used skull models in their investigations, and the use of this gold standard would be valuable to assess whether the linear measurements presently proposed show acceptable reliability and accuracy.

The present study selected patients without TMD symptomatology, for future research it would be valuable to assess, using the methodology proposed, the condyle-fossa relationship of TMD-free patient in comparison with patients suffering with

TMD symptoms. Ideally having a sample with diverse skeletal relationships would be beneficial, in order to assess the differences also within skeletal class I, class II and class III TMD patients.

It can be argued that a possible limitation of the current methodology could lie on the use of maximum intercuspation (MI) for the CBCT imaging acquisition. The patients were asked to have their teeth together into their habitual bite (MI) during the procedure, which may be similar to the centric relation (CR) position. For some patients, however, the difference from CR to MI can be quite large due to dental interferences and cross-bites that create mandible slides from CR to MI to achieve a more comfortable bite position. This is particularly seen in patients with a class III malocclusion, where an edge-to-edge anterior relationship or anterior cross-bite are a common feature, which leads to mandible slides in the forward direction in order to have posterior contact of teeth (Proffit et al, 2008). Class II division 1 malocclusion is another type of malocclusion where large differences can be found from CR to MI position. These patients present a large overjet, and may posture their mandible forward in order to mask this discrepancy (Proffit et al, 2008). This forward slide typical of class II division 1 patients was prevented in the sample used presently, this was done by assuring that the patients had full posterior dental contact before starting image acquisition.

It is possible to infer that the presence of large CR-MI discrepancies sometimes seen in Class III malocclusion patients could lead to a more anterior position of the TMJ condyle within the glenoid fossa. The present results showed no clinically or statistically significant differences in condyle position between the

skeletal class I, class II and class III subjects imaged in MI, thus if the CR-MI discrepancy acted as a significant issue one would expect to see a more anterior position of the class III group, which was not the case.

It may be of value to conduct a study where class III patients are imaged in both CR and MI, in order to evaluate whether or not there is actually a difference in condyle position between those two sometimes quite different occlusal positions. This would however require exposing the patient to twice as much radiation, which it would certainly encounter roadblocks for Ethics Board approval.

A controversial study recently published by Kandasamy, Boeddinghaus & Kruger (2013) found no statistically significant differences in condyle-fossa relationship of TMD-free patients when the mandible was positioned in centric occlusion (CO or maximum intercuspation) and CR. The 19 patients studied using MRI were not specified in terms of skeletal relationship. It was also unclear in this study whether their measurements were conducted in a 3D manner; it is also possible that differences in results could be found if that was not the case. It would be of future research value to conduct a study of the differences in condyle-fossa position in patients with TMD symptoms, as well as patients with class I, class II, and class III skeletal patterns, and assess the condyle position in CO and CR.

Presently, only skeletal class II subjects that showed a class II division 1 dental malocclusion were studied. It would be of research value to also evaluate subjects that present a class II skeletal pattern and a class II division 2 malocclusion, considering the literature reports that this combination may be linked to a more posteriorly positioned condyle within the glenoid fossa likely due to the retroclined

positioning of the upper incisors (Cleall & BeGole, 1982; Owen, 1984; Demisch, Ingervall & Thuer, 1994; Katsavrias & Halazonetis, 2005; Yousefian, Trimble & Folkman, 2006).

Another limitation of the present study is the age range selected, made of both adults and children. Having a more homogeneous sample, with either only growing subjects (children and adolescents), or only non-growing subjects (only adults), would have improved the conclusions drawn presently. This became an issue due to the extensive retrospective evaluation needed to build the sample.

The limited access to acquire a sample of CBCT scans of subjects with different skeletal patterns, as well as the rather strict inclusion criteria set in the methodology, increased the difficult to assess a larger number of patients for the present study. As the aim of this research was assessing the condyle-fossa position in different skeletal patterns, the methodology sample criteria set to include only patients with two or more cephalometric skeletal pattern indicators. This has not been done in previous studies, where either ANB or Wits were assessed, which perhaps allowed other investigators to acquire a larger sample. For future studies on this topic, it would certainly be of value the assessment of a larger sample, as long as the stringent inclusion criteria set by the current study is maintained. The maintenance of strong inclusion criteria, together with a larger sample size would be the perfect combination in the assessment of condyle-fossa relationship in different skeletal patterns.

Chapter V

Conclusion

Based on the results of the present study the following conclusions can be made:

1. The three-dimensional analysis of the TMJ proposed is statistically sufficiently reproducible between the same rater in different time-points, and between different raters, and therefore suitable for use in clinical settings and future research. There is however the matter of operator error and error related to the imaging itself, which should be taken into account when this method is used;
2. There is no statistically significant difference in the three-dimensional position of the TMJ condyle in relation to the glenoid fossa in the different types of skeletal patterns studied. Except for statistical significant differences for the following measurements:
    a. Significantly larger left anterior joint space for the class II group in comparison to class I group;
    b. Significantly larger left fossa depth for the class I group in comparison to the class III group;

    These differences although statistically significant were smaller than 1mm.
3. Although there was a tendency for the AJS to be smaller than the PJS when the measurement means were evaluated, statistical analysis evidenced no statistically significant differences between the anterior, superior and posterior

joint spaces. This shows that there was non-concentricity of the condyle for all the groups studied, however no particular direction was statistically significantly favored. It is unclear whether the differences found would be clinically significant, considering anatomical individual variations. It would be best to assess the condyle-fossa differences in terms of percentage of joint space in future research.

References

Abboud M., Guirado J.L.C., Orentlicher G., & Wahl G. (2013). Comparison of the Accuracy of Cone Beam Computed Tomography and Medical Computed Tomography: Implications for Clinical Diagnostics with Guided Surgery. *International Journal of Oral and Maxillofacial Implants*, 28, 536–542.

ADA - The American Dental Association Council on Scientific Affairs. (2012). The use of cone-beam computed tomography in dentistry - An advisory statement from the American Dental Association Council on Scientific Affairs. *Journal of the American Dental Association*, 143(8), 899-902.

Alexander S.R., Moore R.N., & DuBois L.M. (1993). Mandibular condyle position: comparison of articulator mountings and magnetic resonance imaging. *American Journal of Orthodontics and Dentofacial Orthopedics*, 104, 230-239.

Almasan O.C., Hedesiu M., Baciut G., Leucuta D.C., & Baciut M. (2013). Disk and joint morphology variations on coronal and sagittal MRI in temporomandibular joint disorders. *Clinical Oral Investigation*, 17, 1243-1250.

Angelopoulos C., Scarfe W.C., & Farman A.G. (2012). A Comparison of Maxillofacial CBCT and Medical CT. *Atlas of Oral Maxillofacial Surgery of Clinics of North America,* 20: 1–17.

Athanasiou A.E. (1995). *Orthodontic Cephalometry.* Chicago: Mosby.

Barghan S., Tetradis S., & Mallya S.M. Application of cone beam computed tomography for assessment of the temporomandibular joints. (2012). *Australian Dental Journal,* 57 (1 Suppl), 109–118.

Blaschke D., & Blaschke T. (1981). Normal TMJ bony relationship in centric occlusion. *Journal of Dental Research,* 60, 98-104.

Boeddinghaus R., Whyte A. (2013). Computed tomography of the temporomandibular joint. *Journal of Medical Imaging and Radiation Oncology*, 57(4), 448-454.

Bonilla-Aragon H., Tallents R.H., Katzberg R.W., Kyrkanides S., & Moss M.A. (1999). Condyle position as a predictor of temporomandibular joint internal derangement. *Journal of Prosthetic Dentistry*, 82, 205-8.

Brand J.W., Whinery Jr J.G., Anderson Q.N., & Keenan K.M. Condyle position as a predictor of temporomandibular joint internal derangement. *Oral Surgery Oral Medicine Oral Pathology Journal,* 67, 469-476.

Braun S. (1996). Achieving improved visualization of the temporomandibular joint condyle and fossa in the sagittal cephalogram and a pilot study of their relationships in habitual occlusion. *American Journal of Orthodontics and Dentofacial Orthopedics,* 109, 635-8.

Brown A.A., Scarfe W.C., Scheetz J.P., Silveira A.M., & Farman A.G. (2009). Linear accuracy of cone beam CT derived 3D images. *Angle Orthodontist,* 79, 150-157.

Cleall J.F., & BeGole E.A. Diagnosis and treatment of Class II, Division 2 malocclusion. *Angle Orthodontist,* 52, 38-60.

Cohlmia J.T., Ghosh J., Sinha P.K., Nanda R.S., & Currier G.F. Tomographic assessment of temporomandibular joints in patients with malocclusion. *Angle Orthodontist,* 66, 27-36.

Cortina J.M. What is coefficient alpha? (1993). An examination of theory and applications. *Journal of Applied Psychology,* 78(1), 98-104.

Costa A.L.F., Yasuda C.L., Appenzeller S., Lopes S.L.P.C., & Cendes F. (2008). Comparison of conventional MRI and 3D reconstruction for evaluation of the temporomandibular joint. *Surgical Radiologic Anatomy,* 30, 663-67.

Dalili Z., Khaki N., Kia S.J., & Salamat F. (2012). Assessing joint space and condylar position in the people with normal function of temporomandibular joint with cone-beam computed tomography. *Journal of Dental Research,* 9, 607-12.

Danforth R.A., Dus I., & Mah J. (2003). 3-D volume imaging for dentistry: a new dimension. Journal of the Californian Dental Association, 31, 817-823.

De Leeuw R. (Ed). (2008). *Orofacial Pain – Guidelines for assessment, diagnosis, and management.* 4Ed. Hanover Park: Quintessence Books.

Demisch A., Ingervall B., & Thuer U. Mandibular displacement in Angle Class II, Division 2 malocclusion. (1992). *American Journal of Orthodontics and Dentofacial Orthopedics,* 102, 509-518.

Endo M., Terajima M., Goto TK., Tokumori K., & Takahashi I. (2011). Three-dimensional analysis of the temporomandibular joint and fossa-condyle relationship. *Orthodontics Journal,* 12, 210-221.

Fraga, M.R.; Rodrigues A.F.; Ribeiro L.C.; Campos M.J.S.; Vitral R.W.F. (2013). Anteroposterior condylar position: A comparative study between subjects with normal occlusion and patients with class I, class II division 1, and class III malocclusions. *Medical Science Monitor*, 19, 903-907.

Fuyamada M., Nawa H., Shibata M., Yoshida K., Kise Y., Katsumata A., Ariji E., & Goto S. Reproducibility of landmark identification in the jaw and teeth on 3-dimensional cone-beam computed tomography images – A preliminary study of tentative methods compared to those based on cephalometric definitions. *Angle Orthodontist,* 81, 843-849.

Gribel B.F., Gribel M.N., Frazao D.C., McNamara J.A., & Manzi F.R. (2011). Accuracy and reliability of craniometric measurements on lateral cephalometry and 3D measurements on CBCT scans. *Angle Orthodontist.* 81, 26–35.

Hashem D., Brown J.E., Patel S., Mannocci F., Donaldson A.N., Watson T.F., & Banerjee A. (2013). An In Vitro Comparison of the Accuracy of Measurements Obtained from High- and Low-resolution Cone-beam Computed Tomography Scans. *Journal of Endodontics*, 39, 394–397.

Hashimoto K, Kawashima S, Kameoka S, Akiyama Y., Honjoya T., Ejima K., & Sawada K. (2007). Comparison of image validity between cone beam

computed tomography for dental use and multidetector row helical computed tomography. *Dentomaxillofacial Radiology*, 36, 465-471.

Hintze H, Wiese M, & Wenzel A. Cone beam CT and conventional tomography for the detection of morphological temporomandibular joint changes. (2007). *Dentomaxillofacial Radiology*, 36, 192-197.

Honda K., Larheim T.A., Maruhashi K., Matsumoto K., & Iwai K. (2006). Osseous abnormalities of the mandibular condyle: Diagnostic reliability of cone beam computed tomography compared with helical computed tomography based on an autopsy material. *Dentomaxillofacial Radiology*, 35, 152-157.

Honey O.B., Scarfe W.C., Hilgers M.J., Klueber K., Silveira A.M., Haskell B.S., & Farman A.G. (2007). Accuracy of cone-beam computed tomography imaging of the temporomandibular joint: Comparisons with panoramic radiology and linear tomography. *American Journal of Orthodontics and Dentofacial Orthopedics*, 132(4), 429-438.

Ikeda K., & Kawamura A. (2009). Assessment of optimal condylar position with limited cone-beam computed tomography. *American Journal of Orthodontics and Dentofacial Orthopedics,* 135, 495-501.

Ikeda K., Kawamura A., & Ikeda R. (2011). Assessment of Optimal Condylar Position in the Coronal and Axial Planes with Limited Cone-Beam Computed Tomography. *Journal of Prosthodontics,* 20, 432–438.

Ikeda K., & Kawamura A. (2013). Disc displacement and changes in condylar position. *Dentomaxillofacial Radiology*, 42(3), 84227642.

Kandasamy S., Boeddinghaus R., & Krueger E. (2013). Condylar position assessed by magnetic resonance imaging after various bite position registrations. *American Journal of Orthodontics and Dentofacial Orthopedics,*144, 512-507.

Katsavrias E.G., & Halazonetis D.J. (2005) Condyle and fossa shape in Class II and Class III skeletal patterns: a morphometric tomographic study. *American Journal of Orthodontics and Dentofacial Orthopedics*,128, 337-346.

Krisjane Z., Urtane I., Krumina G., & Zepa K. (2009). Three-dimensional evaluation of TMJ parameters in Class II and Class III patients. *Baltic Dental and Maxillofacial Journal*, 11, 32-36.

Lagravere M.O., Gordon J.M., Guedes I.H., Flores-Mir C., Carey J.P., Heo G., & Major P.W. (2009). Reliability of traditional cephalometric landmarks as seen

in three-dimensional analysis in maxillary expansion treatments. *Angle Orthodontist,* 79, 1047–1056.

Landis J.R., & Koch G.G. (1977). The measurement of observer agreement for categorical data. *Biometrics*, 33, 159-74.

Laskin DM, Greene CS, Hylander WL. (Eds). (2006) *TMDs: An Evidence-Based Approach to Diagnosis and Treatment.* Chicago: Quintessence; 2006.

Ludlow J.B., Davies-Ludlow L.E., & Brooks S.L. (2003). Dosimetry of two extraoral direct digital imaging devices: NewTom cone beam CT and orthophos plus DS panoramic unit. *Dentomaxillofacial Radiology*, 32, 229-234.

Ludlow J.B., Davies-Ludlow L.E., & White S.C. (2007). Patient risk related to common dental radiographic examinations: the impact of 2007 International Commission on Radiological Protection recommendations regarding dose calculation. *Journal of the American Dental Association*, 139(9), 1237-1243.

Ljungquist T.,Harms-Ringdahl K., Nygren A., & Jensen I. (1999). Intra- and inter-rater reliability of an 11-test package for assessing dysfunction due to back or neck pain. *Physiotherapy Research International*, 4, 214-232.

Mischkowski R.A., Pulsfort R., Ritter L., Neugebauer J., Brochhagen H.G., & Keeve E. (2007). Geometric accuracy of a newly developed cone-beam device for maxillofacial imaging. *Oral Surgery Oral Medicine Oral Pathology Oral Radiology and Endodontics*, 104, 551-559.

Moaddab M.B., Dumas A.L., Chavoor A.G., Neff P.A., & Homayoun N. (1985). Temporomandibular joint: computed tomographic three-dimensional reconstruction. *American Journal of Orthodontics*, 88, 342-352.

Mongini F. (1977). Anatomical and clinical evaluation of the relationship between the temporomandibular joint and occlusion. *Journal of Prosthetic Dentistry*, 38, 539-51.

Morant J.J., Salvado M., Hernandez-Giron I., Casanovas R., Ortega R., & Calzado A. (2013). Dosimetry of a cone beam CT device for oral and maxillofacial radiology using Monte Carlo techniques and ICRP adult reference computational phantoms. *Dentomaxillofacial Radiology*, 42, 92555893.

Mozzo P., Procacci C., Tacconi A., Martini P.T., & Andreis I.A. (1998). A new volumetric CT machine for dental imaging based on the cone-beam technique: preliminary results. *European Journal of Radiology*, 8, 1558–1564.

Muller R., & Buttner P. (1994). A critical discussion of intra-class correlation coefficients. *Statistical Medicine,* 13, 2465-76.

Naeije M., Te Veldhuis A.H., Te Veldhuis E.C., Visscher C.M., & Lobbezoo F. (2013). Disc displacement within the human temporomandibular joint: a systematic review of a 'noisy annoyance'. *Journal of Oral Rehabilitation,* 40, 139-158.

Norton N.S. (2007). *Netter's Head and Neck Anatomy for Dentistry.* Philadelphia: Saunders Elsevier.

Okeson J.P. (2008). *Management of Temporomandibular Disorders and Occlusion.* 6th ed. St. Louis: Mosby Elsevier.

Owen A.H. (1984). Orthodontic/orthopedic treatment of craniomandibular pain dysfunction. Part 2: posterior condylar displacement. *Journal of Craniomandibular Practice,* 2, 334-49.

Parks E.T. (2000). Computed tomography applications for dentistry. *Dental Clinics of North America,* 44, 371-394.

Patcas R., Markic G., Muller L., Ullrich O., Peltomaki T., Kellenberger C.J., & Karlo C.A. (2012). Accuracy of linear intraoral measurements using cone beam CT

and multidetector CT: a tale of two CTs. *Dentomaxillofacial Radiology*, 41, 637–644.

Pauwels R., Theodorakou C., Walker A., Bosmans H., Jacobs R., Horner K., & Bogaerts R. (2012). Dose distribution for dental cone bean CT and its implications for defining dose index. *Dentomaxillofacial Radiology*, 41, 583-593.

Pereira L.J., & Gaviao M.B.D. (2004). Tomographic evaluation of TMJ in adolescents with temporomandibular disorders. *Brazilian Oral Research*, 18(3), 208214.

Periago D.R., Scarfe W.C., Moshiri M., Scheetz J.P., Silveira A.M., Farman A.G. Linear accuracy and reliability of cone-beam CT derived 3-dimentional images constructed using an orthodontic volumetric rendering program. *Angle Orthodontist*, 78, 387--395.

Proffit W.R., Fields H.W., & Sarver DM. (Eds). (2007). *Contemporary Orthodontics.* 4 ed. St. Louis: Mosby Elsevier.

Pullinger A.G., & Hollender L. (1985). Assessment of mandibular condyle position: A comparison of transcranial radiographs and linear tomograms. *Oral Surgery Oral Medicine Oral Pathology*, 60, 329-334.

Pullinger A.G., & Hollander L. (1986). Variation in condyle-fossa relationships according to different methods of evaluation of tomograms. *Oral Surgery Oral Medicine Oral Pathology*, 62(6), 719-727.

Pullinger A.G., Seligman D.A., & Gornbein J.A. (1993). A multiple logistic regression analysis of the risk and relative odds of temporomandibular disorders as a function of common occlusal features. *Journal of Dental Research*, 72, 968-979.

Rodrigues A.F., Vitral R.W.F., & Fraga M.R. (2009). Computed tomography evaluation of the temporomandibular joint in Class I malocclusion patients: condylar symmetry and condyle-fossa relationship. *American Journal of Orthodontics and Dentofacial Orthopedics*, 136, 192-198.

Rodrigues A.F., Fraga M.R., & Vitral R.W.F. (2009). Computed tomography evaluation of the temporomandibular joint in Class II Division 1 and in Class III malocclusion patients: condylar symmetry and condyle-fossa relationship. *American Journal of Orthodontics and Dentofacial Orthopedics*, 136, 199-206.

Saccucci M., D'Attilio M., Rodolfino D., Festa F., Polimeni A. & Tecco S. (2012). Condylar volume and condylar area in class I, class II and class III young adult subjects. *Head Face Med,* 8:34-40.

Scarfe W.C., & Farman A.G. (2008). What is cone-beam CT and how does it work? *Dental Clinics of North America,* 52, 707-730.

Schilling R., & Geibel M.A. (2013). Assessment of the effective doses from two dental cone beam CT devices. *Dentomaxillofacial Radiology,* 42, 20120273.

Schulze D., Heiland M., Thurmann H., & Adam G. (2004). Radiation exposure during midfacial imaging using 4- and 16-slice computed tomography, cone beam computed tomography systems and conventional radiography. *Dentomaxillofacial Radiology,* 33, 83-86.

Seren E., Akan H., Toller M.O., & Seren A. (1994). An evaluation of the condylar position of the temporomandibular joint by computerized tomography in Class III malocclusions: A preliminary study. *American Journal of Orthodontics and Dentofacial Orthopedics*, 136105, 483-8.

Sharout P. (1998). Measurement reliability and agreement in psychiatry. *Statistical Methods in Medical Research,* 7, 301-317.

Smith S.R., Matteson S.R., Phillips C., & Tyndall D.A. (1989). Quantitative and subjective analysis of temporomandibular joint radiographs. *Journal of Prosthetic Dentistry,* 62, 456-63.

Stamm T., Hohoff A., Van Meegen A., & Meyer U. (2004). On the Three-Dimensional Physiological Position of the Temporomandibular Joint. *Journal of Orofacial Orthopedics,* 65, 280–289.

Sumbullu M.A., Caglayan F., Akgul H.M., & Yilmaz A.B. (2012). Radiological examination of the articular eminence morphology using cone beam CT. *Dentomaxillofacial Radiology*, 41, 234–240.

Suomalainen A., Vehmas T., Kortesniemi M., Robinson S., & Peltola J. (2008). Accuracy of linear measurements using dental cone beam and conventional multislice computed tomography. *Dentomaxillofacial Radiology,* 37, 10-17.

Tanaka E., Hirose M., & Koolstra J.H. (2008). Modeling of the effect of friction in the temporomandibular joint on displacement of its disc during prolonged clenching. *Journal of Oral Maxillofacial Surgery,* 66, 462-468.

The SEDENTEXCT Project. (2013, May 5). *Radiation Protection: Cone Beam CT for Dental and Maxillofacial Radiology: Evidence Based Guidelines 2011).* Retrieved May 5, 2013 from www.sedentexct.eu/files/guidelines_final.pdf.

Tsiklakis K., Syriopoulos K., & Stamatakis H.C. (2004). Radiographic examination of the temporomandibular joint using cone beam computed tomography. *Dentomaxillofacial Radiology,* 33, 196-201.

Tyndall D.A., Renner J.B., Phillips C., & Matteson S.R. (1992). Positional Changes of the Mandibular Condyle Assessed by Three-Dimensional Computed Tomography. *Journal of Oral and Maxillofacial Surgery,* 50, 1164-72.

Vitral R.W.F., & Telles C.S. (2002). Computed tomography evaluation of temporomandibular joint alterations in Class II Division 1 subdivision patients: condylar symmetry. *American Journal of Orthodontics and Dentofacial Orthopedics,* 121,369-375.

Vitral R.W.F, Telles C.S., Fraga M.R., Oliveira R.S.M.F., & Tanaka O.M. (2004) Computed tomography evaluation of temporomandibular joint alterations in patients with Class II Division 1 subdivision malocclusions: condyle-fossa relationship. *American Journal of Orthodontics and Dentofacial Orthopedics,* 126, 48-52.

Vitral R.W.F., Campos M.J.S., Rodrigues A.F., & Fraga, M.R. (2011). Temporomandibular joint and normal occlusion: Is there anything singular

about it? A computed tomographic evaluation. *American Journal of Orthodontics and Dentofacial Orthopedics*, 40, 18-24.

Weinberg L.A. (1979). Role of the condylar position in TMJ dysfunction syndrome. *Journal of Prosthetic Dentistry*, 41, 636-643.

Zain-Alabdeen E.H., & Alsadhan R.I. (2012). A comparative study of accuracy of detection of surface osseous changes in the temporomandibular joint using multidetector CT and cone beam CT. *Dentomaxillofacial Radiology*, 41, 185–191.

Zamora N., Llamas J., Cibrian R., Gandia J., Paredes V. (2012). A study on the reproducibility of cephalometric landmarks when undertaking a three-dimensional (3D) cephalometric analysis. *Medicina Oral Patologia Oral Cirurgia Bucal*, 17, 678-688.

Appendix 1

Ethics Approval – University of Manitoba

P126 - 770 Bannatyne Avenue
Winnipeg, Manitoba
Canada R3E 0W3
Tel: (204) 789-3255
Fax: (204) 789-3414

UNIVERSITY of MANITOBA | BANNATYNE CAMPUS Research Ethics Boards

APPROVAL FORM

Principal Investigator: Dr. I. Guedes
Supervisor: Dr. M. Lagravere

Ethics Reference Number: H2012:086
Date of Approval: April 2, 2012
Date of Expiry: April 2, 2013

Protocol Title: **Three dimensional evaluation of the temporomandibular joint condyle position in different malocclusions using cone-beam computerized tomography**

The following is/are approved for use:

- **Proposal submitted March 6, 2012**
- **Data Capture Sheet submitted March 6, 2012**

The above underwent delegated review and was **approved as submitted** on April 2, 2012 by Dr. John Arnett, Ph.D., C. Psych., Health Research Ethics Board, Bannatyne Campus, University of Manitoba on behalf of the committee per your submission dated March 30, 2012. The Research Ethics Board is organized and operates according to Health Canada/ICH Good Clinical Practices, Tri-Council Policy Statement, and the applicable laws and regulations of Manitoba. The membership of this Research Ethics Board complies with the membership requirements for Research Ethics Boards defined in Division 5 of the *Food and Drug Regulations of Canada*.

This approval is valid for one year only. A study status report must be submitted annually and must accompany your request for re-approval. Any significant changes of the protocol and informed consent form should be reported to the Chair for consideration in advance of implementation of such changes. The REB must be notified regarding discontinuation or study closure.

This approval is for the ethics of human use only. For the logistics of performing the study, approval must be sought form the relevant institution, if required.

Sincerely yours,

[redacted]

John Arnett, Ph.D., C. Psych.
Chair, Health Research Ethics Board
Bannatyne Campus

Please quote the above Ethics Reference Number on all correspondence.
Inquiries should be directed to REB Secretary
Telephone: (204) 789-3255 / Fax: (204) 789-3414

www.umanitoba.ca/medicine/ethics

Ethics Approval – University of Alberta

View: Study - Pro00013379

Exit | Hide/Show Errors| Print... | Jump To:

Reviewer Notes *(0 Notes Total)*

Help

VIEW000072

ID:Pro00013379

Status: Approved

1.1 Study Identification

*All questions preceded by a red asterisk * are required fields. Other fields may be required by the REB in order to evaluate your application.*

Please answer all presented questions that will reasonably help to describe your study or proposed research.

1.0 * **Short Study Title** *(restricted to 250 characters)***:**

Three dimensional evaluation of the temporomandibular joint condyle position

2.0 * **Long Study Title** *(can be exactly the same as short title)***:**

Three dimensional evaluation of the temporomandibular joint condyle position

3.0 * **Select the appropriate Research Ethics Board:**

HREB Biomedical

4.0 * **Which office requires notification of ethics approval to release funds or finalize the study contract?** *(It is the PI's responsibility to provide ethics approval notification to any office other than the ones listed below)*

Not applicable

5.0 * **Name of Principal Investigator** *(at the University of Alberta, Covenant Health, or Alberta Health Services)***:**

Manuel Lagravere Vich

Appendix 2

Statistical Analysis Tables

Table 3 Intra-reliability's Inter-item correlation matrix (x-axis)

landmarks		x1	x2	x3
1.00	x1	1.00	1.00	1.00
	x2	1.00	1.00	1.00
	x3	1.00	1.00	1.00
2.00	x1	1.00	1.00	1.00
	x2	1.00	1.00	1.00
	x3	1.00	1.00	1.00
3.00	x1	1.00	1.00	1.00
	x2	1.00	1.00	1.00
	x3	1.00	1.00	1.00
4.00	x1	1.00	1.00	1.00
	x2	1.00	1.00	1.00
	x3	1.00	1.00	1.00
5.00	x1	1.00	1.00	1.00
	x2	1.00	1.00	1.00
	x3	1.00	1.00	1.00
6.00	x1	1.00	1.00	1.00
	x2	1.00	1.00	1.00
	x3	1.00	1.00	1.00
7.00	x1	1.00	1.00	1.00
	x2	1.00	1.00	1.00
	x3	1.00	1.00	1.00
8.00	x1	1.00	1.00	1.00
	x2	1.00	1.00	1.00
	x3	1.00	1.00	1.00
9.00	x1	1.00	1.00	1.00
	x2	1.00	1.00	1.00
	x3	1.00	1.00	1.00
10.00	x1	1.00	.99	1.00
	x2	.99	1.00	.99
	x3	1.00	.99	1.00
11.00	x1	1.00	.99	1.00
	x2	.99	1.00	.99
	x3	1.00	.99	1.00

12.00	x1	1.00	1.00	1.00
	x2	1.00	1.00	1.00
	x3	1.00	1.00	1.00
13.00	x1	1.00	1.00	1.00
	x2	1.00	1.00	1.00
	x3	1.00	1.00	1.00
14.00	x1	1.00	.99	1.00
	x2	.99	1.00	.99
	x3	1.00	.99	1.00
15.00	x1	1.00	1.00	1.00
	x2	1.00	1.00	1.00
	x3	1.00	1.00	1.00
16.00	x1	1.00	1.00	1.00
	x2	1.00	1.00	1.00
	x3	1.00	1.00	1.00
17.00	x1	1.00	1.00	1.00
	x2	1.00	1.00	1.00
	x3	1.00	1.00	1.00
18.00	x1	1.00	1.00	1.00
	x2	1.00	1.00	1.00
	x3	1.00	1.00	1.00

Table 4 Intra-reliability's Intra class correlation coefficient (ICC) for x-axis

landmarks		Intraclass Correlation	95% Confidence Interval		F Test with True Value 0			
			Lower Bound	Upper Bound	Value	df1	df2	Sig
1.00	Single Measures	1.00	1.00	1.00	164886.12	9	18	.00
	Average Measures	1.00	1.00	1.00	164886.12	9	18	.00
2.00	Single Measures	1.00	.99	1.00	13515.95	9	18	.00
	Average Measures	1.00	1.00	1.00	13515.95	9	18	.00
3.00	Single Measures	1.00	.99	1.00	10342.55	9	18	.00
	Average Measures	1.00	1.00	1.00	10342.55	9	18	.00
4.00	Single Measures	1.00	.99	1.00	14196.04	9	18	.00
	Average Measures	1.00	1.00	1.00	14196.04	9	18	.00
5.00	Single Measures	1.00	1.00	1.00	295253.49	9	18	.00
	Average Measures	1.00	1.00	1.00	295253.79	9	18	.00
6.00	Single Measures	1.00	1.00	1.00	26041.86	9	18	.00
	Average Measures	1.00	1.00	1.00	26041.68	9	18	.00
7.00	Single Measures	1.00	1.00	1.00	20717.03	9	18	.00
	Average Measures	1.00	1.00	1.00	20717.03	9	18	.00
8.00	Single Measures	1.00	.99	1.00	11842.91	9	18	.00
	Average Measures	1.00	1.00	1.00	11842.91	9	18	.00
9.00	Single Measures	1.00	.99	1.00	15181.13	9	18	.00
	Average Measures	1.00	1.00	1.00	15181.13	9	18	.00
10.00	Single Measures	.99	.99	.99	1341.80	9	18	.00
	Average Measures	.99	.99	1.00	1341.80	9	18	.00
11.00	Single Measures	.99	.99	1.00	3258.57	9	18	.00
	Average Measures	1.00	.99	1.00	3258.57	9	18	.00
12.00	Single Measures	1.00	.99	1.00	13430.31	9	18	.00
	Average Measures	1.00	1.00	1.00	13430.31	9	18	.00
13.00	Single Measures	1.00	.99	1.00	10258.96	9	18	.00
	Average Measures	1.00	1.00	1.00	10258.96	9	18	.00
14.00	Single Measures	.99	.99	1.00	3502.07	9	18	.00
	Average Measures	1.00	.99	1.00	3502.07	9	18	.00
15.00	Single Measures	1.00	1.00	1.00	38908.51	9	18	.00
	Average Measures	1.00	1.00	1.00	38908.51	9	18	.00
16.00	Single Measures	1.00	.99	1.00	12323.64	9	18	.00
	Average Measures	1.00	1.00	1.00	12323.64	9	18	.00
17.00	Single Measures	1.00	.99	1.00	13112.88	9	18	.00
	Average Measures	1.00	1.00	1.00	13112.88	9	18	.00
18.00	Single Measures	1.00	.99	1.00	7776.24	9	18	.00
	Average Measures	1.00	1.00	1.00	7776.24	9	18	.00

Table 5 Intra-reliability's Cronbach's alpha statistics (y-axis)

landmarks	Cronbach's Alpha	Cronbach's Alpha Based on Standardized Items	N of Items
1.00	1.00	1.00	3
2.00	1.00	1.00	3
3.00	1.00	1.00	3
4.00	1.00	1.00	3
5.00	1.00	1.00	3
6.00	1.00	1.00	3
7.00	1.00	1.00	3
8.00	1.00	1.00	3
9.00	1.00	1.00	3
10.00	.99	.99	3
11.00	1.00	1.00	3
12.00	1.00	1.00	3
13.00	1.00	1.00	3
14.00	1.00	1.00	3
15.00	1.00	1.00	3
16.00	1.00	1.00	3
17.00	1.00	1.00	3
18.00	1.00	1.00	3

Table 6 Intra-reliability's Inter-item correlation matrix (y-axis)

landmarks		y1	y2	y3
1.00	y1	1.00	1.00	1.00
	y2	1.00	1.00	1.00
	y3	1.00	1.00	1.00
2.00	y1	1.00	1.00	1.00
	y2	1.00	1.00	1.00
	y3	1.00	1.00	1.00
3.00	y1	1.00	1.00	1.00
	y2	1.00	1.00	1.00
	y3	1.00	1.00	1.00
4.00	y1	1.00	1.00	1.00
	y2	1.00	1.00	1.00
	y3	1.00	1.00	1.00
5.00	y1	1.00	1.00	1.00
	y2	1.00	1.00	1.00
	y3	1.00	1.00	1.00
6.00	y1	1.00	1.00	1.00
	y2	1.00	1.00	1.00
	y3	1.00	1.00	1.00
7.00	y1	1.00	1.00	1.00
	y2	1.00	1.00	1.00
	y3	1.00	1.00	1.00
8.00	y1	1.00	1.00	1.00
	y2	1.00	1.00	1.00
	y3	1.00	1.00	1.00
9.00	y1	1.00	1.00	1.00
	y2	1.00	1.00	1.00
	y3	1.00	1.00	1.00
10.00	y1	1.00	.99	1.00
	y2	.99	1.00	.99
	y3	1.00	.99	1.00
11.00	y1	1.00	1.00	1.00
	y2	1.00	1.00	1.00
	y3	1.00	1.00	1.00
12.00	y1	1.00	1.00	1.00
	y2	1.00	1.00	1.00
	y3	1.00	1.00	1.00
13.00	y1	1.00	.99	1.00
	y2	.99	1.00	.99

	y3	1.00	.99	1.00
14.00	y1	1.00	1.00	1.00
	y2	1.00	1.00	1.00
	y3	1.00	1.00	1.00
15.00	y1	1.00	1.00	1.00
	y2	1.00	1.00	1.00
	y3	1.00	1.00	1.00
16.00	y1	1.00	1.00	1.00
	y2	1.00	1.00	1.00
	y3	1.00	1.00	1.00
17.00	y1	1.00	1.00	1.00
	y2	1.00	1.00	.99
	y3	1.00	.99	1.00
18.00	y1	1.00	1.00	1.00
	y2	1.00	1.00	1.00
	y3	1.00	1.00	1.00

Table 7 Intra-reliability's Intra class correlation coefficient (ICC) for y-axis

landmarks		Intraclass Correlation	95% Confidence Interval		F Test with True Value 0			
			Lower Bound	Upper Bound	Value	df1	df2	Sig
1	Single Measures	1.00	.99	1.00	11597.43	9	18	.00
	Average Measures	1.00	1.00	1.00	11597.43	9	18	.00
2	Single Measures	1.00	1.00	1.00	24579.57	9	18	.00
	Average Measures	1.00	1.00	1.00	24579.57	9	18	.00
3	Single Measures	1.00	.99	1.00	15987.57	9	18	.00
	Average Measures	1.00	1.00	1.00	15987.57	9	18	.00
4	Single Measures	1.00	1.00	1.00	37580.18	9	18	.00
	Average Measures	1.00	1.00	1.00	37580.18	9	18	.00
5	Single Measures	1.00	1.00	1.00	42305.86	9	18	.00
	Average Measures	1.00	1.00	1.00	42305.86	9	18	.00
6	Single Measures	1.00	.99	1.00	12230.44	9	18	.00
	Average Measures	1.00	1.00	1.00	12230.44	9	18	.00
7	Single Measures	1.00	1.00	1.00	20264.52	9	18	.00
	Average Measures	1.00	1.00	1.00	20264.52	9	18	.00
8	Single Measures	.99	.99	1.00	6064.60	9	18	.00
	Average Measures	1.00	1.00	1.00	6064.60	9	18	.00
9	Single Measures	.99	.98	.99	746.77	9	18	.00
	Average Measures	.99	.99	1.00	746.77	9	18	.00
10	Single Measures	.99	.99	1.00	2523.17	9	18	.00
	Average Measures	1.00	.99	1.00	2523.17	9	18	.00

11	Single Measures	1.00	.99	1.00	8584.19	9	18	.00
	Average Measures	1.00	1.00	1.00	8584.19	9	18	.00
12	Single Measures	.99	.99	1.00	4317.15	9	18	.00
	Average Measures	1.00	.99	1.00	4317.15	9	18	.00
13	Single Measures	.99	.99	1.00	4941.86	9	18	.00
	Average Measures	1.00	.99	1.00	4941.86	9	18	.00
14	Single Measures	1.00	.99	1.00	11694.12	9	18	.00
	Average Measures	1.00	1.00	1.00	11694.22	9	18	.00
15	Single Measures	1.00	1.00	1.00	26365.07	9	18	.00
	Average Measures	1.00	1.00	1.00	26365.07	9	18	.00
16	Single Measures	1.00	1.00	1.00	31721.94	9	18	.00
	Average Measures	1.00	1.00	1.00	31721.94	9	18	.00
17	Single Measures	1.00	.99	1.00	7517.74	9	18	.00
	Average Measures	1.00	1.00	1.00	7517.74	9	18	.00
18	Single Measures	1.00	.99	1.00	13745.31	9	18	.00
	Average Measures	1.00	.99	1.00	13745.30	9	18	.00

Table 8 Intra-reliability's Cronbach's alpha statistics (y-axis)

Landmarks	Cronbach's Alpha	Cronbach's Alpha Based on Standardized Items	N of Items
1	1.00	1.00	3
2	1.00	1.00	3
3	1.00	1.00	3
4	1.00	1.00	3
5	1.00	1.00	3
6	1.00	1.00	3
7	1.00	1.00	3
8	1.00	1.00	3
9	.99	1.00	3
10	1.00	1.00	3
11	1.00	1.00	3
12	1.00	1.00	3
13	1.00	1.00	3
14	1.00	1.00	3
15	1.00	1.00	3
16	1.00	1.00	3
17	1.00	1.00	3
18	1.00	1.00	3

Table 9 Intra-reliability's Inter-item correlation matrix (z-axis)

landmarks		z1	z2	z3
1	z1	1.00	1.00	1.00
	z2	1.00	1.00	1.00
	z3	1.00	1.00	1.00
2	z1	1.00	1.00	1.00
	z2	1.00	1.00	1.00
	z3	1.00	1.00	1.00
3	z1	1.00	1.00	1.00
	z2	1.00	1.00	1.00
	z3	1.00	1.00	1.00
4	z1	1.00	1.00	1.00
	z2	1.00	1.00	1.00
	z3	1.00	1.00	1.00
5	z1	1.00	1.00	1.00
	z2	1.00	1.00	1.00
	z3	1.00	1.00	1.00
6	z1	1.00	1.00	1.00
	z2	1.00	1.00	1.00
	z3	1.00	1.00	1.00
7	z1	1.00	1.00	1.00
	z2	1.00	1.00	1.00
	z3	1.00	1.00	1.00
8	z1	1.00	1.00	1.00
	z2	1.00	1.00	1.00
	z3	1.00	1.00	1.00
9	z1	1.00	1.00	1.00
	z2	1.00	1.00	1.00
	z3	1.00	1.00	1.00
10	z1	1.00	1.00	1.00
	z2	1.00	1.00	1.00
	z3	1.00	1.00	1.00
11	z1	1.00	1.00	1.00
	z2	1.00	1.00	1.00
	z3	1.00	1.00	1.00
12	z1	1.00	1.00	1.00
	z2	1.00	1.00	1.00
	z3	1.00	1.00	1.00
13	z1	1.00	.99	.99
	z2	.99	1.00	.99

	z3	.99	.99	1.00
14	z1	1.00	1.00	1.00
	z2	1.00	1.00	1.00
	z3	1.00	1.00	1.00
15	z1	1.00	1.00	1.00
	z2	1.00	1.00	1.00
	z3	1.00	1.00	1.00
16	z1	1.00	1.00	1.00
	z2	1.00	1.00	1.00
	z3	1.00	1.00	1.00
17	z1	1.00	1.00	1.00
	z2	1.00	1.00	1.00
	z3	1.00	1.00	1.00
18	z1	1.00	1.00	.99
	z2	1.00	1.00	1.00
	z3	.99	1.00	1.00

Table 10 Intra-reliability's Intra class correlation coefficient (ICC) for z-axis

Landmarks		Intraclass Correlation	95% Confidence Interval		F Test with True Value 0			
			Lower Bound	Upper Bound	Value	df1	df2	Sig
1	Single Measures	1.00	1.00	1.00	33297.56	9	18	.00
	Average Measures	1.00	1.00	1.00	33297.56	9	18	.00
2	Single Measures	1.00	1.00	1.00	29768.20	9	18	.00
	Average Measures	1.00	1.00	1.00	29768.20	9	18	.00
3	Single Measures	1.00	1.00	1.00	207096.35	9	18	.00
	Average Measures	1.00	1.00	1.00	207096.35	9	18	.00
4	Single Measures	1.00	.99	1.00	12519.74	9	18	.00
	Average Measures	1.00	1.00	1.00	12519.74	9	18	.00
5	Single Measures	1.00	1.00	1.00	26010.52	9	18	.00
	Average Measures	1.00	1.00	1.00	26010.52	9	18	.00
6	Single Measures	1.00	1.00	1.00	104501.20	9	18	.00
	Average Measures	1.00	1.00	1.00	104501.27	9	18	.00
7	Single Measures	1.00	1.00	1.00	52157.28	9	18	.00
	Average Measures	1.00	1.00	1.00	52157.28	9	18	.00
8	Single Measures	1.00	.99	1.00	8223.04	9	18	.00
	Average Measures	1.00	1.00	1.00	8223.04	9	18	.00
9	Single Measures	1.00	.99	1.00	10433.93	9	18	.00
	Average Measures	1.00	1.00	1.00	10433.93	9	18	.00
10	Single Measures	1.00	1.00	1.00	58435.44	9	18	.00
	Average Measures	1.00	1.00	1.00	58435.44	9	18	.00

11	Single Measures	.99	.99	1.00	6411.27	9	18	.00
	Average Measures	1.00	1.00	1.00	6411.27	9	18	.00
12	Single Measures	1.00	.99	1.00	11375.06	9	18	.00
	Average Measures	1.00	1.00	1.00	11375.06	9	18	.00
13	Single Measures	.99	.99	1.00	4362.79	9	18	.00
	Average Measures	1.00	.99	1.00	4362.79	9	18	.00
14	Single Measures	1.00	.99	1.00	8698.16	9	18	.00
	Average Measures	1.00	1.00	1.00	8698.16	9	18	.00
15	Single Measures	1.00	1.00	1.00	165588.01	9	18	.00
	Average Measures	1.00	1.00	1.00	165588.05	9	18	.00
16	Single Measures	1.00	1.00	1.00	47452.31	9	18	.00
	Average Measures	1.00	1.00	1.00	47452.31	9	18	.00
17	Single Measures	1.00	1.00	1.00	24444.24	9	18	.00
	Average Measures	1.00	1.00	1.00	24444.24	9	18	.00
18	Single Measures	.99	.99	1.00	6326.13	9	18	.00
	Average Measures	1.00	.99	1.00	6326.13	9	18	.00

Table 11 Intra-reliability's Cronbach's alpha statistics (z-axis)

landmarks	Cronbach's Alpha	Cronbach's Alpha Based on Standardized Items	N of Items
1	1.00	1.00	3
2	1.00	1.00	3
3	1.00	1.00	3
4	1.00	1.00	3
5	1.00	1.00	3
6	1.00	1.00	3
7	1.00	1.00	3
8	1.00	1.00	3
9	1.00	1.00	3
10	1.00	1.00	3
11	1.00	1.00	3
12	1.00	1.00	3
13	1.00	1.00	3
14	1.00	1.00	3
15	1.00	1.00	3
16	1.00	1.00	3
17	1.00	1.00	3
18	1.00	1.00	3

Table 12 Inter-reliability's Inter-item correlation matrix (x-axis)

Landmarks		x2	mx	jx
1	x2	1.00	1.00	1.00
	mx	1.00	1.00	1.00
	jx	1.00	1.00	1.00
2	x2	1.00	1.00	1.00
	mx	1.00	1.00	1.00
	jx	1.00	1.00	1.00
3	x2	1.00	1.00	1.00
	mx	1.00	1.00	1.00
	jx	1.00	1.00	1.00
4	x2	1.00	1.00	1.00
	mx	1.00	1.00	1.00
	jx	1.00	1.00	1.00
5	x2	1.00	1.00	1.00
	mx	1.00	1.00	1.00
	jx	1.00	1.00	1.00
6	x2	1.00	1.00	1.00
	mx	1.00	1.00	1.00
	jx	1.00	1.00	1.00
7	x2	1.00	1.00	1.00
	mx	1.00	1.00	1.00
	jx	1.00	1.00	1.00
8	x2	1.00	1.00	1.00
	mx	1.00	1.00	1.00
	jx	1.00	1.00	1.00
9	x2	1.00	1.00	1.00
	mx	1.00	1.00	1.00
	jx	1.00	1.00	1.00
10	x2	1.00	.99	.99
	mx	.99	1.00	1.00
	jx	.99	1.00	1.00
11	x2	1.00	.99	.99
	mx	.99	1.00	1.00
	jx	.99	1.00	1.00
12	x2	1.00	1.00	1.00
	mx	1.00	1.00	1.00
	jx	1.00	1.00	1.00
13	x2	1.00	1.00	1.00
	mx	1.00	1.00	1.00

	jx	1.00	1.00	1.00
14	x2	1.00	.99	1.00
	mx	.99	1.00	1.00
	jx	1.00	1.00	1.00
15	x2	1.00	1.00	1.00
	mx	1.00	1.00	1.00
	jx	1.00	1.00	1.00
16	x2	1.00	1.00	1.00
	mx	1.00	1.00	1.00
	jx	1.00	1.00	1.00
17	x2	1.00	1.00	1.00
	mx	1.00	1.00	1.00
	jx	1.00	1.00	1.00
18	x2	1.00	1.00	1.00
	mx	1.00	1.00	1.00
	jx	1.00	1.00	1.00

Table 13 Inter-reliability's Intra class correlation coefficient (ICC) for x-axis

Landmarks		Intraclass Correlation	95% Confidence Interval		F Test with True Value 0			
			Lower Bound	Upper Bound	Value	df1	df2	Sig
1	Single Measures	1.00	.98	1.00	136745.32	9	18	.00
	Average Measures	1.00	.99	1.00	136745.32	9	18	.00
2	Single Measures	1.00	.99	1.00	16048.51	9	18	.00
	Average Measures	1.00	.99	1.00	16048.51	9	18	.00
3	Single Measures	1.00	.99	1.00	19686.17	9	18	.00
	Average Measures	1.00	.99	1.00	19686.17	9	18	.00
4	Single Measures	1.00	.99	1.00	17864.76	9	18	.00
	Average Measures	1.00	1.00	1.00	17864.76	9	18	.00
5	Single Measures	1.00	.99	1.00	216603.15	9	18	.00
	Average Measures	1.00	.99	1.00	216603.15	9	18	.00
6	Single Measures	1.00	.99	1.00	20593.34	9	18	.00
	Average Measures	1.00	.99	1.00	20593.34	9	18	.00
7	Single Measures	1.00	.99	1.00	55237.27	9	18	.00
	Average Measures	1.00	.99	1.00	55237.27	9	18	.00
8	Single Measures	1.00	.99	1.00	15065.22	9	18	.00
	Average Measures	1.00	.99	1.00	15065.22	9	18	.00
9	Single Measures	.99	.98	1.00	28658.28	9	18	.00
	Average Measures	1.00	.99	1.00	28658.28	9	18	.00
10	Single Measures	.99	.99	1.00	2744.64	9	18	.00
	Average Measures	1.00	.99	1.00	2744.64	9	18	.00

11	Single Measures	1.00	.99	1.00	7713.64	9	18	.00
	Average Measures	1.00	1.00	1.00	7713.64	9	18	.00
12	Single Measures	.99	.99	1.00	19012.28	9	18	.00
	Average Measures	1.00	.99	1.00	19012.28	9	18	.00
13	Single Measures	1.00	.99	1.00	30348.20	9	18	.00
	Average Measures	1.00	.99	1.00	30348.20	9	18	.00
14	Single Measures	.99	.99	1.00	7486.79	9	18	.00
	Average Measures	1.00	.99	1.00	7486.79	9	18	.00
15	Single Measures	.99	.81	.99	13554.41	9	18	.00
	Average Measures	.99	.92	1.00	13554.41	9	18	.00
16	Single Measures	1.00	.99	1.00	13600.99	9	18	.00
	Average Measures	1.00	1.00	1.00	13600.99	9	18	.00
17	Single Measures	1.00	.99	1.00	46670.80	9	18	.00
	Average Measures	1.00	.99	1.00	46670.80	9	18	.00
18	Single Measures	.99	.99	1.00	13897.26	9	18	.00
	Average Measures	1.00	.99	1.000	13897.261	9	18	.00

Table 14 Inter-reliability's Cronbach's alpha statistics (x-axis)

Landmarks	Cronbach's Alpha	Cronbach's Alpha Based on Standardized Items	N of Items
1	1.00	1.00	3
2	1.00	1.00	3
3	1.00	1.00	3
4	1.00	1.00	3
5	1.00	1.00	3
6	1.00	1.00	3
7	1.00	1.00	3
8	1.00	1.00	3
9	1.00	1.00	3
10	1.00	1.00	3
11	1.00	1.00	3
12	1.00	1.00	3
13	1.00	1.00	3
14	1.00	1.00	3
15	1.00	1.00	3
16	1.00	1.00	3
17	1.00	1.00	3
18	1.00	1.00	3

Table 15 Inter-reliability's Inter-item correlation matrix (y-axis)

landmarks		y2	my	jy
1	y2	1.00	.99	.99
	my	.99	1.00	.99
	jy	.99	.99	1.00
2	y2	1.00	.99	.99
	my	.99	1.00	.99
	Jy	.99	.99	1.00
3	y2	1.00	.99	.99
	my	.99	1.00	.99
	jy	.99	.99	1.00
4	y2	1.00	.99	.99
	my	.99	1.00	.99
	jy	.99	.99	1.00
5	y2	1.00	.99	.99
	my	.99	1.00	.99
	jy	.99	.99	1.00
6	y2	1.00	.99	.99
	my	.99	1.00	.99
	jy	.99	.99	1.00
7	y2	1.00	.99	.99
	my	.99	1.00	.99
	jy	.99	.99	1.00
8	y2	1.00	.99	.99
	my	.99	1.00	.99
	jy	.99	.99	1.00
9	y2	1.00	.99	.99
	my	.99	1.00	.99
	jy	.99	.99	1.00
10	y2	1.00	.99	.99
	my	.99	1.00	.99
	jy	.99	.99	1.00
11	y2	1.00	.99	.99
	my	.99	1.00	.99
	jy	.99	.99	1.00
12	y2	1.00	.99	.99
	my	.99	1.00	.99
	jy	.99	.99	1.00
13	y2	1.00	.99	.99
	my	.99	1.00	.99

	jy	.99	.99	1.00
14	y2	1.00	.99	.99
	my	.99	1.00	.99
	jy	.99	.99	1.00
15	y2	1.00	.99	.99
	my	.99	1.00	.99
	jy	.99	.99	1.00
16	y2	1.00	.99	.99
	my	.99	1.00	.99
	jy	.99	.99	1.00
17	y2	1.00	.99	.99
	my	.99	1.00	.99
	jy	.99	.99	1.00
18	y2	1.00	.99	.99
	my	.99	1.00	.99
	jy	.99	.99	1.00

Table 16 Inter-reliability's Intra class correlation coefficient (ICC) for y-axis

Landmarks		Intraclass Correlation	95% Confidence Interval		F Test with True Value 0			
			Lower Bound	Upper Bound	Value	df1	df2	Sig
1	Single Measures	.99	.99	.99	1221.14	9	18	.00
	Average Measures	.99	.99	1.00	1221.14	9	18	.00
2	Single Measures	.99	.99	.99	1790.64	9	18	.00
	Average Measures	.99	.99	1.00	1790.64	9	18	.00
3	Single Measures	.99	.99	.99	1213.72	9	18	.00
	Average Measures	.99	.99	1.00	1213.72	9	18	.00
4	Single Measures	.99	.99	1.00	2002.58	9	18	.00
	Average Measures	.99	.99	1.00	2002.58	9	18	.00
5	Single Measures	.99	.99	.99	1299.07	9	18	.00
	Average Measures	.99	.99	1.00	1299.07	9	18	.00
6	Single Measures	.99	.99	1.00	1944.19	9	18	.00
	Average Measures	.99	.99	1.00	1944.19	9	18	.00
7	Single Measures	.99	.99	.99	1366.73	9	18	.00
	Average Measures	.99	.99	1.00	1366.73	9	18	.00
8	Single Measures	.99	.99	1.00	2336.42	9	18	.00
	Average Measures	1.00	.99	1.00	2336.42	9	18	.00
9	Single Measures	.99	.99	.99	1175.60	9	18	.00
	Average Measures	.99	.99	1.00	1175.60	9	18	.00
10	Single Measures	.99	.99	1.00	1887.51	9	18	.00
	Average Measures	.99	.99	1.00	1887.51	9	18	.00
11	Single	.99	.99	.99	1369.19	9	18	.00

	Measures							
	Average Measures	.99	.99	1.00	1369.19	9	18	.00
12	Single Measures	.99	.99	1.00	2248.48	9	18	.00
	Average Measures	1.00	.99	1.00	2248.48	9	18	.00
13	Single Measures	.99	.99	.99	1347.22	9	18	.00
	Average Measures	.99	.99	1.00	1347.22	9	18	.00
14	Single Measures	.99	.99	1.00	2063.87	9	18	.00
	Average Measures	1.00	.99	1.00	2063.87	9	18	.00
15	Single Measures	.99	.99	.99	1219.14	9	18	.00
	Average Measures	.99	.99	1.00	1219.14	9	18	.00
16	Single Measures	.99	.99	.99	1920.74	9	18	.00
	Average Measures	.99	.99	1.00	1920.74	9	18	.00
17	Single Measures	.99	.99	.99	1134.02	9	18	.00
	Average Measures	.99	.99	1.00	1134.02	9	18	.00
18	Single Measures	.99	.99	.99	1824.11	9	18	.00
	Average Measures	.99	.99	1.00	1824.11	9	18	.00

Table 17 Inter-reliability's Cronbach's alpha statistics (y-axis)

Landmarks	Cronbach's Alpha	Cronbach's Alpha Based on Standardized Items	N of Items
1	.99	.99	3
2	.99	.99	3
3	.99	.99	3
4	1.00	1.00	3
5	.99	.99	3
6	.99	1.00	3
7	.99	.99	3
8	1.00	1.00	3
9	.99	.99	3
10	.99	1.00	3
11	.99	.99	3
12	1.00	1.00	3
13	.99	.99	3
14	1.00	1.00	3
15	.99	.99	3
16	.99	1.00	3
17	.99	.99	3
18	.99	.99	3

Table 18 Inter-reliability's Inter-item correlation matrix (z-axis)

landmarks		z2	mz	jz
1	z2	1.00	.99	1.00
	mz	.99	1.00	.99
	jz	1.00	.99	1.00
2	z2	1.00	.99	.99
	mz	.99	1.0	.9
	jz	.99	.99	1.00
3	z2	1.00	.99	1.00
	mz	.99	1.00	.99
	jz	1.00	.99	1.00
4	z2	1.00	.99	.99
	mz	.99	1.00	.99
	jz	.99	.9	1.00
5	z2	1.00	.99	1.00
	mz	.99	1.00	.99
	jz	1.00	.99	1.00
6	z2	1.00	.99	.99
	mz	.99	1.00	.99
	jz	.99	.99	1.00
7	z2	1.00	.99	.99
	mz	.99	1.00	.99
	jz	.99	.99	1.00
8	z2	1.00	.99	.99
	mz	.99	1.00	1.0
	jz	.99	1.00	1.00
9	z2	1.00	.99	.99
	mz	.99	1.00	1.00
	jz	.99	1.00	1.00
10	z2	1.00	.99	.99
	mz	.99	1.00	.99
	jz	.99	.99	1.00
11	z2	1.00	.99	.99
	mz	.99	1.00	.99
	jz	.99	.99	1.00
12	z2	1.00	1.00	1.00
	mz	1.00	1.00	.99
	jz	1.00	.99	1.00
13	z2	1.00	.99	1.00
	mz	.99	1.00	.99

	jz	1.00	.99	1.00
14	z2	1.00	.99	.99
	mz	.99	1.00	.99
	jz	.99	.99	1.00
15	z2	1.00	.99	.99
	mz	.99	1.00	.99
	jz	.99	.99	1.00
16	z2	1.00	.99	.99
	mz	.99	1.00	.99
	jz	.99	.99	1.00
17	z2	1.00	1.00	1.00
	mz	1.00	1.00	.99
	jz	1.00	.99	1.00
18	z2	1.00	.99	.99
	mz	.99	1.00	.99
	jz	.99	.99	1.00

Table 19 Inter-reliability's Intra class correlation coefficient (ICC) for z-axis

Landmarks		Intraclass Correlation	95% Confidence Interval		F Test with True Value 0			
			Lower Bound	Upper Bound	Value	df1	df2	Sig
1	Single Measures	.99	.99	1.00	2713.69	9	18	.00
	Average Measures	1.00	.99	1.00	2713.69	9	18	.00
2	Single Measures	.99	.99	1.00	3054.14	9	18	.00
	Average Measures	1.00	.99	1.00	3054.14	9	18	.00
3	Single Measures	.99	.99	1.00	3856.81	9	18	.00
	Average Measures	1.00	.99	1.00	3856.81	9	18	.00
4	Single Measures	.99	.99	1.00	2896.19	9	18	.00
	Average Measures	1.00	.99	1.00	2896.19	9	18	.00
5	Single Measures	.99	.99	1.00	3222.57	9	18	.00
	Average Measures	1.00	.99	1.00	3222.57	9	18	.00
6	Single Measures	.99	.99	1.00	3118.53	9	18	.00
	Average Measures	1.00	.99	1.00	3118.53	9	18	.00
7	Single Measures	.99	.99	1.00	2790.18	9	18	.00
	Average Measures	1.00	.99	1.00	2790.18	9	18	.00
8	Single Measures	.81	.57	.94	14.27	9	18	.00
	Average Measures	.93	.80	.98	14.27	9	18	.00
9	Single Measures	.55	.17	.84	4.66	9	18	.00
	Average Measures	.78	.39	.94	4.66	9	18	.00
10	Single Measures	.99	.99	1.00	4052.53	9	18	.00
	Average Measures	1.00	.99	1.00	4052.53	9	18	.00
11	Single	.99	.99	1.00	3131.79	9	18	.00

	Measures							
	Average Measures	1.00	.99	1.00	3131.79	9	18	.00
12	Single Measures	.99	.99	1.00	5489.45	9	18	.00
	Average Measures	1.00	.99	1.00	5489.45	9	18	.00
13	Single Measures	.99	.99	1.00	3565.27	9	18	.00
	Average Measures	1.00	.99	1.00	3565.27	9	18	.00
14	Single Measures	.99	.99	1.00	3274.96	9	18	.00
	Average Measures	1.00	.99	1.00	3274.96	9	18	.00
15	Single Measures	.99	.99	1.00	3338.13	9	18	.00
	Average Measures	1.00	.99	1.00	3338.13	9	18	.00
16	Single Measures	.99	.99	1.00	3033.96	9	18	.00
	Average Measures	1.00	.99	1.00	3033.96	9	18	.00
17	Single Measures	.99	.99	1.00	3895.73	9	18	.00
	Average Measures	1.00	.99	1.00	3895.73	9	18	.00
18	Single Measures	.99	.99	1.00	3056.17	9	18	.00
	Average Measures	1.00	.99	1.00	3056.17	9	18	.00

Table 20 Inter-reliability's Cronbach's alpha statistics (z-axis)

landmarks	Cronbach's Alpha	Cronbach's Alpha Based on Standardized Items	N of Items
1	1.00	1.00	3
2	1.00	1.00	3
3	1.00	1.00	3
4	1.00	1.00	3
5	1.00	1.00	3
6	1.00	1.00	3
7	1.00	1.00	3
8	.93	.99	3
9	.78	.99	3
10	1.00	1.00	3
11	1.00	1.00	3
12	1.00	1.00	3
13	1.00	1.00	3
14	1.00	1.00	3
15	1.00	1.00	3
16	1.00	1.00	3
17	1.00	1.00	3
18	1.00	1.00	3

Table 25 Descriptive statistics – mean values and standard deviation

Class		Mean	Std. Deviation	N
1	AJS-L	3.48	1.17	30
	AJS-R	3.23	.90	30
	SJS-L	3.82	1.33	30
	SJS-R	3.68	1.35	30
	PJS-L	4.45	1.47	30
	PJS-R	4.48	1.52	30
	CA-L	104.20	10.57	30
	CA-R	103.81	8.60	30
	FA-L	109.86	13.45	30
	FA-R	111.95	11.60	30
	FD-L	5.08	.94	30
	FD-R	5.21	.70	30
	Total	38.60	49.22	360
2	AJS-L	4.29	1.19	30
	AJS-R	3.53	.99	30
	SJS-L	4.24	1.32	30
	SJS-R	4.10	1.57	30
	PJS-L	4.79	1.41	30
	PJS-R	4.80	1.86	30
	CA-L	100.08	13.15	30
	CA-R	103.17	9.61	30
	FA-L	113.79	11.40	30
	FA-R	115.23	14.58	30
	FD-L	4.88	.89	30
	FD-R	5.03	.91	30
	Total	39.00	49.56	360
3	AJS-L	3.76	.90	30
	AJS-R	3.59	.94	30
	SJS-L	3.54	.97	30
	SJS-R	3.55	.90	30
	PJS-L	4.63	1.21	30
	PJS-R	4.29	1.07	30
	CA-L	101.65	8.22	30
	CA-R	102.31	8.95	30
	FA-L	114.30	14.93	30
	FA-R	113.68	11.89	30
	FD-L	4.33	.90	30
	FD-R	4.78	.96	30

	Total	38.70	49.60	360
Total	AJS-L	3.85	1.14	90
	AJS-R	3.45	.94	90
	SJS-L	3.87	1.24	90
	SJS-R	3.78	1.31	90
	PJS-L	4.62	1.36	90
	PJS-R	4.52	1.51	90
	CA-L	101.98	10.85	90
	CA-R	103.10	8.98	90
	FA-L	112.65	13.33	90
	FA-R	113.62	12.69	90
	FD-L	4.76	.96	90
	FD-R	5.00	.87	90
	Total	38.77	49.42	1080

Table 27 Multiple comparisons between variables and groups - Post-hoc test - Bonferroni

Measure			Mean Diff.	Std. Error	Sig.	95% Confidence Interval	
						Lower Bound	Upper Bound
AJS-L	1	2	-.81	.28	**.016**	-1.50	-.11
		3	-.28	.28	.97	-.97	.41
	2	1	.81	.28	**.016**	.11	1.50
		3	.53	.28	.19	-.16	1.22
	3	1	.28	.28	.97	-.41	.97
		2	-.53	.28	.19	-1.22	.16
AJS-R	1	2	-.30	.24	.63	-.90	.28
		3	-.36	.24	.43	-.95	.23
	2	1	.30	.24	.63	-.28	.90
		3	-.05	.24	1.00	-.64	.54
	3	1	.36	.24	.43	-.23	.95
		2	.05	.24	1.00	-.54	.64
SJS-L	1	2	-.41	.31	.57	-1.18	.35
		3	.28	.31	1.00	-.48	1.05
	2	1	.41	.31	.57	-.35	1.18
		3	.69	.31	.09	-.07	1.46
	3	1	-.28	.31	1.00	-1.05	.48
		2	-.69	.31	.09	-1.46	.07
SJS-R	1	2	-.42	.33	.62	-1.25	.39
		3	.12	.33	1.00	-.69	.94
	2	1	.42	.33	.62	-.39	1.25
		3	.55	.33	.31	-.27	1.37
	3	1	-.12	.33	1.00	-.94	.69
		2	-.55	.33	.31	-1.37	.27
PJS-L	1	2	-.34	.35	1.00	-1.20	.52
		3	-.17	.35	1.00	-1.04	.68
	2	1	.34	.35	1.00	-.52	1.20
		3	.16	.35	1.00	-.69	1.03
	3	1	.17	.35	1.00	-.68	1.04
		2	-.16	.35	1.00	-1.03	.69
PJS-R	1	2	-.31	.39	1.00	-1.27	.64
		3	.19	.39	1.00	-.76	1.15
	2	1	.31	.39	1.00	-.64	1.27
		3	.51	.39	.58	-.44	1.47

	3	1	-.19	.39	1.00	-1.15	.76
		2	-.51	.39	.58	-1.47	.44
CA-L	1	2	4.11	2.79	.43	-2.71	10.95
		3	2.55	2.79	1.00	-4.27	9.38
	2	1	-4.11	2.79	.43	-10.95	2.71
		3	-1.56	2.79	1.00	-8.39	5.23
	3	1	-2.55	2.79	1.00	-9.38	4.27
		2	1.56	2.79	1.00	-5.26	8.39
CA-R	1	2	.64	2.34	1.00	-5.07	6.35
		3	1.50	2.34	1.00	-4.21	7.21
	2	1	-.64	2.34	1.00	-6.35	5.07
		3	.85	2.34	1.00	-4.85	6.57
	3	1	-1.50	2.34	1.00	-7.21	4.21
		2	-.85	2.34	1.00	-6.57	4.85
FA-L	1	2	-3.93	3.44	.76	-12.34	4.47
		3	-4.44	3.44	.60	-12.85	3.96
	2	1	3.93	3.44	.76	-4.47	12.34
		3	-.50	3.44	1.00	-8.91	7.90
	3	1	4.44	3.46	.60	-3.96	12.85
		2	.50	3.44	1.00	-7.90	8.91
FA-R	1	2	-3.27	3.295	.96	-11.32	4.76
		3	-1.72	3.29	1.00	-9.76	6.32
	2	1	3.27	3.29	.96	-4.76	11.32
		3	1.55	3.29	1.00	-6.49	9.59
	3	1	1.72	3.29	1.00	-6.32	9.76
		2	-1.55	3.29	1.00	-9.59	6.49
FD-L	1	2	.19	.23	1.00	-.38	.77
		3	.751	.23	**.006**	.17	1.32
	2	1	-.19	.23	1.00	-.77	.38
		3	.55	.23	.06	-.02	1.13
	3	1	-.751	.23	**.006**	-1.32	-.17
		2	-.55	.23	.06	-1.13	.02
FD-R	1	2	.18	.22	1.00	-.36	.73
		3	.43	.22	.16	-.11	.98
	2	1	-.18	.22	1.00	-.73	.36
		3	.25	.22	.80	-.29	.79
	3	1	-.43	.22	.16	-.98	.11
		2	-.25	.22	.80	-.79	.29